ELSEVIER

Seminars in
NUCLEAR
MEDICINE

Positron Emission Tomography for Prostate, Bladder, and Renal Cancer

Heiko Schöder, MD, and Steven M. Larson, MD

Prostate cancer, renal cancer, bladder, and other urothelial malignancies make up the common tumors of the male genitourinary tract. For prostate cancer, common clinical scenarios include managing the patient presenting with 1) low-risk primary cancer; 2) high-risk primary cancer; 3) prostate-specific antigen (PSA) recurrence after apparently successful primary therapy; 4) progressive metastatic disease in the noncastrate state; and 5) progressive metastatic disease in the castrate state. These clinical states dictate the appropriate choice of diagnostic imaging modalities. The role of positron emission tomography (PET) is still evolving but is likely to be most important in determining early spread of disease in patients with aggressive tumors and for monitoring response to therapy in more advanced patients. Available PET tracers for assessment of prostate cancer include FDG, ^{11}C or ^{18}F choline and acetate, ^{11}C methionine, ^{18}F fluoride, and fluorodihydrotestosterone. Proper staging of prostate cancer is particularly important in high-risk primary disease before embarking on radical prostatectomy or radiation therapy. PET with ^{11}C choline or acetate, but not with FDG, appears promising for the assessment of nodal metastases. PSA relapse frequently is the first sign of recurrent or metastatic disease after radical prostatectomy or radiation therapy. PET with FDG can identify local recurrence and distant metastases, and the probability for a positive test increases with PSA. However, essentially all studies have shown that the sensitivity for recurrent disease detection is higher with either acetate or choline as compared with FDG. Although more data need to be gathered, it is likely that these two agents will become the PET tracers of choice for staging prostate cancer once metastatic disease is strongly suspected or documented. ^{18}F fluoride may provide a more sensitive bone scan and will probably be most valuable when PSA is greater than 20 ng/mL in patients with high suspicion or documented osseous metastases. Several studies suggest that FDG uptake in metastatic prostate cancer lesions reflects the biologic activity of the disease. Accordingly, FDG can be used to monitor the response to chemotherapy and hormonal therapy. Androgen receptor imaging agents like fluorodihydrotestosterone are being explored to predict the biology of treatment response for progressive tumor in late stage disease in castrated patients. The assessment of renal masses and primary staging of renal cell carcinoma are the domain of helical CT. PET with FDG may be helpful in the evaluation of "equivocal findings" on conventional studies, including bone scan, and also in the differentiation between recurrence and posttreatment changes. The value of other PET tracers in renal cell carcinoma is under investigation. Few studies have addressed the role of PET in bladder cancer. Because of its renal excretion, FDG is not a useful tracer for the detection of primary bladder tumors. The few studies that investigated its role in the detection of lymph node metastases at the time of primary staging were largely disappointing. Bladder cancer imaging with ^{11}C choline, ^{11}C methionine, or ^{11}C- acetate deserves further study.
Semin Nucl Med 34:274-292

Prostate cancer is the most common malignancy among men in the United States, accounting for approximately one third of all cancer diagnoses. Approximately 230,000 new cases of prostate cancer will be diagnosed in 2004.[1] Nowadays prostate cancer is most commonly diagnosed by prostate-specific antigen (PSA) screening. The tumor has a variable biology, ranging from low-grade indolent cancers to aggressive tumors that inexorably spread and kill the patient principally by metastatic involvement of bone marrow and bone.

Prostate cancers vary widely in their rate of growth, aggressiveness, and tendency to metastasize. The biology of this disease evolves from a small, slow-growing, androgen-dependent "indolent" carcinoma toward a more and more aggressive, androgen-independent tumor during the course of progression.[2,3] Recently,

Department of Radiology/Nuclear Medicine, Memorial Sloan-Kettering Cancer Center, New York, NY.
Address reprint requests to: Heiko Schöder, MD, Department of Radiology/Nuclear Medicine, Memorial Sloan-Kettering Cancer Center, 1275 York Avenue, New York, NY 10021.

 0001-2998/04/$-see frontmatter
doi:10.1053/j.semnuclmed.2004.06.004

Scher and coworkers have described this concept of "clinical states" that helps stratify patients for management.[4] The states model notes individual patient status as primary tumor, PSA relapse, noncastrate metastases, and castrate metastases. It seems to us that this clinical-states model also could provide a framework for recommendations for appropriate diagnostic imaging in a given clinical scenario. For example, positron emission tomography (PET) imaging is unlikely to be useful in indolent primary tumors, but PET may be useful in more aggressive primary tumors with a high risk of local extension and metastatic involvement.

In the United States, three important practice patterns dominate diagnosis and management of prostate cancer: 1) the widespread use of serum assays for PSA during routine health surveillance, followed by ultrasound directed biopsies of the prostate, has led to early diagnosis of prostate cancer. Therefore, more than 70% of prostate cancers are now diagnosed when the tumor is organ confined, and radical prostatectomy, brachytherapy, or external beam radiation are used with curative intent. 2) In individual patients, nomograms are used as an aid to management decisions by predicting the likely pathological stage of the disease and the probability of recurrence and metastases after treatment with curative intent. These nomograms combine information from PSA, Gleason score at biopsy, and clinical stage at presentation. 3) Prostate cancer, either primary or metastatic, almost always is responsive to androgen withdrawal (medical or surgical castration). For this reason, patients with more aggressive tumors are likely to receive treatment with antiandrogens early in the course of their disease. Such therapy is likely to have an important impact on functional imaging tests such as PET.

Primary Prostate Cancer

As for other malignancies, the primary staging is important in patients with prostate cancer, especially in the more aggressive local tumors. The extent of prostate cancer should be determined as accurately as possible to direct therapy rationally based on the clinical stage and to evaluate the prognosis. Both the clinical stage of the disease and the probability for nonlocalized disease (extracapsular extension, seminal vesicle invasion, nodal disease) will determine the choice of therapy.

Greater than 75% of patients with newly diagnosed prostate cancer now present with clinically localized disease. Hence, the diagnostic yield of imaging studies in an unselected group of prostate cancer patients would be very low. Instead, functional imaging studies particularly are likely be most meaningful in the more aggressive primary lesions. Therefore, rather than uniformly applying a certain test in all patients, specific imaging studies should be based on the clinical state of the patient. This decision could be based on commonly used tables or nomograms for presurgical risk stratification.[5-7] Nomograms usually combine PSA, Gleason score,[8] and clinical stage to predict the pathologic stage of the disease[5] or incorporate data from surgical pathology to predict the probability for PSA relapse and survival.[9] The nomograms are considerably more accurate than any of the clinical parameters in isolation. For instance, using the clinical examination alone, the true stage of prostate cancer will be underestimated in as many as 30% to 60% of patients.[10] By definition, however, nomograms only indicate a certain likelihood for organ-confined disease, but they do not provide exact staging information in the individual patient.[5,9,11] Therefore, it would be desirable to have an accurate, noninvasive staging tool, which then should be applied in selected groups of patients (eg, high risk for nonorgan-confined disease based on nomogram).

Role of Conventional Imaging Studies for Primary Staging

Transrectal ultrasound (TRUS) is the most commonly used imaging modality for viewing the prostate. However, only 60% of tumors are visualized by TRUS, and the method often is used simply to localize the prostate, as a guide to biopsy. Nonetheless, it is said that in the hands of experts, TRUS detects extracapsular extension with accuracy between 58% and 86%. However, a recent multicenter trial TRUS casts doubt on this statement because TRUS was no more accurate at predicting organ-confined disease than was the digital rectal examination.[12,13]

Computed tomography (CT) lacks soft-tissue contrast resolution for the detection of cancer within the prostate. Its role in the local staging of prostate cancer also is limited because of its low accuracy (24% for extracapsular extension and 69% for seminal vesicle invasion).[14]

In experienced hands, the most accurate imaging test for primary staging is magnetic resonance imaging (MRI) using an endorectal coil in conjunction with a pelvic phased-array coil.[15] Although not perfect, this test can identify and localize the primary tumor and assess for potential extracapsular extension (sensitivity 50%; specificity 95%[16]; and seminal vesicle invasion. In addition, MRI can detect or exclude perineural invasion of tumor with high accuracy,[16] which is an important criterion when nerve-sparing surgery is considered. Overall sensitivity and specificity for the local staging of prostate cancer range between 51% and 89% and 67% and 87% respectively, with accuracy between 54% and 88%.[17,18]

Prostate cancer is associated with characteristic alterations in the concentration of certain metabolites, such as an increase in prostate choline and a decrease in prostate citrate levels, as compared with normal prostate tissue. These metabolic alterations can be detected by magnetic resonance spectroscopy (MRS).[19] The addition of spectroscopy to MRI alone may aid in the detection of prostatic cancer tissue and may increase the specificity of MRI. The addition of MRS to MRI improved staging accuracy significantly when used by an inexperienced reader compared with that by an experienced reader, and the latter was able to further improve the accuracy.[20] However, MRS is sensitive to technical artifacts and currently still considered investigational; it is not yet in widespread use. It also needs to be emphasized that these data from MRI and MRS were generated by a few experienced institutions; it remains to be seen whether the reported high sensitivity and specificity can be reproduced once the technique enjoys widespread use.

Role of PET for Primary Staging

Available PET Tracers for the Imaging of Prostate Cancer and the Biochemical Rationale for Their Use

FDG. PET imaging with [18F] 2-fluoro-D-deoxy-glucose (FDG) takes advantage of the increase in glycolytic flux in cancer cells (Table 1). In rapidly growing, de-differentiated tumors, aerobic glycolysis is increased and respiration decreased.[21] Even under aerobic conditions, as much as 50% of the ATP produced in tumor cells is derived from glycolysis (in contrast to approximately 10% in normal cells, which mostly rely on oxidative phosphorylation as a source for energy). Increased glycolysis is associated with quantitative and qualitative changes in enzyme expression and activities, glucose transporter molecules, as well as cytoskeletal arrangements. Some of these processes have been studied in prostate cancer. In vitro (cell cultures), rapidly dividing DU145 prostate cancer cells depend on high levels of glucose consumption, whereas relatively slow-growing LNCaP cells were found to be less dependent on glucose.[22] Glucose can be used for the synthesis of ATP and as a

Table 1 Characteristics and Suggested Applications of PET Tracers for Imaging of Prostate Cancer

	^{18}F FDG	^{11}C Methionine	^{11}C Choline	^{18}F Choline	^{11}C Acetate	^{18}F FDHT
Normal biodistribution	Myocardium, bowel, liver, spleen, kidney	Pancreas, liver, spleen, kidney, salivary glands	Lung, liver, kidney, adrenal	Renal cortex, liver, spleen, salivary glands	Lung, spleen, pancreas, liver, kidney (mild in BM and bowel)	Liver, blood pool, small intestine (excr.)
Primary mode of excretion	Renal	Urinary	Intestinal	Urinary	Intestinal	Intestinal
Urinary activity?	+++	++	+	++*	Minimal†	–
Suitable for						
Detection of primary PCA	–	–	–	–	–	–
Primary staging (LN, mets)	–	?	+	?	+	–
PSA relapse						
Local recurrence	(+)§	?	+++	++	+++	–
Distant metastases	+	++	+++	+++	+++	–
Prognostic value?	+	?	?	?	?	Likely
Therapy monitoring?	++	?	?	?	?	+
Typical activity in mCi (MBq)	370–555	370–555	370–925	185–260	555–925	370–555
Imaging start at min p.i.	45–60	5–10	5	3	5–10	Dynamic: immed. static: 60 min
EDE in mSv/MBq	2×10^{-2}	5×10^{-3}‡	5×10^{-3}	3.5×10^{-2}‖	6.2×10^{-3}¶	No data

EDE, effective dose equivalent.
*Beginning at 5 min p.i.
†Kato et al.[53]
‡Deloar et al.[179]
§When using a combined PET/CT.
‖DeGrado et al.[72]
¶Seltzer et al.[180]

precursor for DNA synthesis. Glucose also serves as a substrate for the synthesis of diacylglycerol, which is a ligand for protein kinase C (the latter plays an important role in cellular signal transduction.[23] Although no clear relationship between these biochemical alteration and FDG uptake in prostate cancer has been demonstrated, they do provide the rationale for the hypothesis that FDG may selectively detect more aggressive tumors, which depend on higher glucose metabolism. Indeed, in vitro studies in prostate cancer xenografts showed higher FDG uptake in tumors with higher Gleason score,[24] and in clinical studies FDG uptake correlates with PSA level and PSA velocity as measures of tumor size and progression.[25-27]

The initial results of prostate cancer imaging with FDG were disappointing.[28,29] These negative results were likely related to four factors: 1) limited sensitivity of FDG for prostate cancer lesions; 2) urinary excretion of FDG with tracer activity in ureters and bladder, making it difficult to distinguish lymph nodes or local recurrence; 3) use of older image reconstruction techniques, leading to streak artifacts in the pelvis[30]; and 4) the lack of appropriate patient selection.

However, despite its poor reputation from earlier reports, FDG is in fact not an unsuitable tracer for the investigation of prostate carcinoma but needs to be used in carefully selected groups of patients.[27,31-34] It is our belief that the use of adequate imaging techniques (iterative reconstruction, segmented attenuation correction)[35] and especially the application of combined PET-CT imaging can reduce the number of false-negative and false-positive findings.

However, urinary excretion of FDG remains undesirable for examining pelvic malignancies. Other PET tracers, in particular choline and acetate, have therefore been studied in patients with prostate cancer. According to unanimous initial reports these agents hold great promise.

Acetate. Shreve and coworkers introduced ^{11}C-acetate as a potential PET tracer for various malignancies, including prostate cancer.[36,37] In a small group of 18 patients, acetate showed a higher sensitivity than FDG for the detection of local recurrence or metastatic disease. These investigators suggested that the lack of urinary excretion and good tumor:background ratio make acetate a more suitable tracer for imaging of prostate cancer.

During the past few years this tracer also has been used for the imaging of prostate cancer.[26,38,39] Acetate be can also be labeled with ^{18}F fluorine, although methods for safe and efficient synthesis are still under investigation. Preliminary data from animal experiments and one case report suggest that this agent might be useful for imaging of prostate cancer.[40,41]

Acetate uptake in tumor cells is related to lipid synthesis.[42,43] Yoshimoto and coworkers[42] incubated tumor cell lines and fibroblasts with ^{14}C acetate and analyzed the production of $^{14}CO_2$ and other ^{14}C-labeled metabolites. In addition, glucose metabolic rate was assessed with ^{3}H deoxyglucose (DOG) and the cell growth rate by ^{3}H thymidine incorporation into DNA. Tumor cell to nontumor cell ratios were higher for acetate than DOG. ^{14}C acetate was metabolized and incorporated into the cellular lipid pool, mostly phosphatidylcholine (which is a building block for cellular membranes) and neutral lipids. Of note, the amount of ^{14}C in lipids correlated with cellular growth activity as measured by ^{3}H thymidine incorporation. The remaining fraction of ^{14}C acetate was converted into CO_2 and amino acids. Although there were differences between tumor cell lines, in each case at least 70% of the activity was always found in intracellular lipids or amino acids. This is in contrast to the myocardium, where acetate is mainly used for oxidative metabolism.[44-46]

Additional studies in prostate cancer provided the pathophysiologic rationale for the incorporation of acetate into lipids: Normal prostate tissue shows high citrate production and accumulation.[47,48] In prostate cancer, however, citrate content is significantly reduced. In addition, some citrate also is transported from the mitochondrion to cytosol, where it is converted to oxaloacetate and acetyl-CoA.[47] The latter is the building block for fatty acids, which are used for membrane synthesis and metabolism. Other studies demonstrated an increase in fatty acid synthesis and accumulation, as well as

overexpression of the key enzyme fatty acid synthase (FAS) in prostate cancer.[49] This overexpression of FAS occurs early in cancer development and in hormone-responsive tumors (such as prostate cancer) is more pronounced as the tumor progresses toward the more advanced stage.[50] Recent studies have also shown that (^{14}C) acetate is predominantly incorporated into intracellular phosphatidylcholine, that acetate uptake is an indirect measure of the FAS pathway,[43] and that FAS-mediated lipid synthesis mainly affects lipids in membrane rafts[43] (membrane rafts are associated with signal transduction processes)[51,52] that are relevant for tumor growth and metastasis.

Acetate is not a cancer-specific tracer but also accumulates in normal and hyperplastic prostate tissue. In fact, the standardized uptake value (SUV) for ^{11}C-acetate uptake was found to be higher in individuals with normal prostate tissue younger than 50 years of age than in normal prostate of older subjects (>50 years) or those with benign prostatic hypertrophy (BPH).[53] In addition, there was no difference in prostate SUV between older subjects with normal prostate (2.3 ± 0.7) and patients with proven prostate cancer (1.9 ± 0.6). The relationship between intensity of acetate uptake in prostate cancer and PSA and is unclear.[26,39] Although many prostate cancer patients have been studied with ^{11}C-acetate, full papers published to date include only about 150 patients.

Choline. In the human body, choline is needed for the synthesis of phospholipids in cell membranes, methyl metabolism, transmembrane signaling, and lipid–cholesterol transport and metabolism.[54] Intracellular choline is rapidly metabolized to phosphorylcholine (PC); it may also undergo acetylation to form acetylcholine or oxidation to form betaine (mainly in liver and kidney). The phosphorylation is catalyzed by the enzyme choline kinase. Once phosphorylated, the polar PC molecule is trapped within the cell. Various studies have revealed an increased choline uptake as well as an upregulated activity of choline kinase and elevated levels of PC in cancer cells.[55-57] These observations gave rise to the development and clinical evaluation of MRS imaging, which revealed a high content of PC in prostate cancer,[19] whereas in normal tissue this choline metabolite was found in low concentrations or was undetectable.

Based on these observations, Hara and coworkers introduced ^{11}C-choline for the imaging of malignancies[58-61] including prostate carcinoma. The efficacy of radiolabeled choline (labeled to ^{11}C or ^{18}F) for localizing primary or metastatic prostate cancer has now been studied in more than 250 patients.[62-67]

^{11}C-choline blood clearance is very rapid (approximately 7 min), and the major amount of tracer remains trapped within cells. This allows for imaging as early as 3 to 5 min after tracer injection and provides images of good diagnostic quality.[58,59] Physiologically increased tracer uptake is noted in salivary glands, lung, liver, kidneys, and adrenal glands.[68] The short half life time for ^{11}C (20 min) poses a logistic challenge in many institutions. This has been addressed with the recent successful synthesis of ^{18}F-labeled choline compounds. Hara and coworkers[69] synthesized F-18 fluoro-ethyl-choline (FEC) and DeGrado and coworkers synthesized fluoromethyl-dimethyl-2-hydroxyethylammonium (FCH).[70-72] In vitro (cultured PC-3 human prostate cells) studies revealed that cellular uptake and phosphorylation by choline kinase were very similar for FCH and natural choline but were lower for FEC.[71] Both compounds show rapid clearance from the blood pool, appearing in the urinary bladder 3 to 5 min after injection. This is in contrast to ^{11}C choline, which shows very little urinary excretion, the activity concentration in the bladder was always lower than in prostate cancer or metastases.[73] It has been suggested that early urinary appearance of F-18 choline compounds is caused by incomplete tubular reabsorption of intact tracer or by enhanced excretion of oxidized metabolites.[70]

All three labeled choline compounds show rapid clearance from blood pool and rapid uptake in prostate tissue.[69,70,73] FEC concentration in the prostate reaches its highest activity at 55 min p.i. (SUV 4.4 versus 2.8 at 5 min),[69] whereas FCH uptake shows a peak at approximately 3 min p.i. followed by a plateau.[70] It is unclear whether this difference would be clinically relevant because beyond 5 to 8 min p.i., the increasing accumulation of excreted tracer in the urinary bladder exceeds activity in the prostate and may interfere with visualization of abnormalities in the prostate (similar to FDG). Although urinary activity can be eliminated by bladder irrigation, this is neither desirable nor always feasible. Therefore, imaging of the prostate with ^{18}F-labeled choline compounds should probably commence at about 1 min after IV injection (to allow for tracer clearance from the blood pool). Subsequently, as urinary activity increases (which would interfere with visualizing prostate tumors) but blood pool activity is low, images of the remainder of the body can be acquired.

Just like FDG, methionine, or acetate, choline is not a cancer-specific agent. Individuals with BPH show tracer uptake that is higher than in normal prostate tissue and lower than in carcinoma. However, in individual patients the intensity of uptake in the prostate cannot reliably distinguish between benign changes and cancer.[73] Nonspecific uptake of (^{18}F) choline in granulocytes and macrophages[74] and (^{11}C) choline in reactive lymph nodes[66] have also been described.

Intense bowel activity can be observed with all choline compounds and can be a reason for false-positive findings.[64,66] Imaging of the abdomen and pelvis may benefit from fasting, as pancreatic juice and bile both contain PCs (and hence excreted activity). False-negative findings have been described for metastases in lymph nodes of less than 1 cm in size.[64,66]

Currently, it is unclear whether choline uptake in prostate cancer lesions can serve as an indicator of biologic aggressiveness. In at least one study,[73] there was no correlation between SUV of (^{11}C) choline in prostate cancer and tumor grade or Gleason score.

Methionine. ^{11}C-methionine has been used as a tumor imaging agent for several years.[75-78] Its uptake reflects increased amino acid transport and, in part, protein synthesis; it also is related to cellular proliferation activity.[79,80] In cancer, methionine uptake also is correlated with the amount of viable tumor tissue.[81] Nilsson was the first to use this tracer in prostate cancer, reporting promising results in metastatic tumor.[82] Macapinlac and coworkers[83] compared the biodistribution of ^{11}C methionine and FDG in 29 patients with androgen-independent metastatic prostate cancer. Both agents showed good uptake in index lesions. Tumor uptake of methionine occurred faster (peak at around 10 min followed by plateau) than that for FDG (sometimes continued rise >45 min). ^{11}C-methionine undergoes rapid clearance from the blood pool, which is faster than for FDG. Methionine is primarily metabolized in liver and pancreas, but shows no significant renal excretion. This biodistribution may explain why methionine appears to be more successful than FDG in imaging prostate cancer and nodal metastases.[34]

^{18}F Fluorodihydrotestosterone (FDHT). The androgen receptor plays an important role in the proliferation and growth of prostate cancer. Virtually all patients with prostate cancer initially respond to androgen withdrawal, but eventually, the cancer cell will begin to grow, despite continued low levels of androgen. There is growing evidence that the escape from suppression offered by androgen

ablation therapy is related to continued signaling through the androgen receptor.[2,84]

Imaging of the androgen receptor expression and its modulation or occupation by drugs might hence prove useful in treatment monitoring. For this purpose, the group at Washington University, St. Louis, developed the radiotracer 16β-^{18}F-fluoro-5α-dihydrotestosterone (FDHT), which is radiolabeled analog of dihydrotestosterone, the primary ligand of the androgen receptor.[85] Recently, Larson and coworkers[32] studied the biodistribution and binding characteristics of FDHT in seven patients with metastatic prostate cancer. Patients were imaged before and after therapy. Seventy-eight percent of 59 lesions had both FDHT and FDG uptake, and the remainder had FDG but not FDHT uptake. Further work is underway to evaluate this metabolic heterogeneity. Many patients with prostate cancer eventually develop resistance to androgen ablation. It is thought that this development of androgen independence characterizes a more aggressive prostate cancer phenotype. Accordingly, one might speculate that prostate cancer lesions that show FDHT uptake indicate presence of differentiated tumor cells likely to respond to androgen withdrawal. In contrast, lesions with persistent FDG uptake but lack of FDHT uptake might represent a more aggressive, androgen-independent tumor cell clone. This pattern of differential tracer uptake is in analogy to thyroid and breast cancer (inverse relationship between FDG and Iodide uptake or FDG uptake and estrogen receptor binding). Studies are ongoing to further elucidate the clinical usefulness of FDHT in certain subgroups of prostate cancer patients.

Clinical Results for Diagnosis and Local Staging With PET. Early studies investigating the role of PET with FDG in primary prostate cancer produced disappointing results.[28,29] In contrast to other malignancies, most primary prostate carcinomas show relatively low FDG uptake. Small size, slow doubling time (2–4 years in most cases) and specifics of prostate metabolism (see above) might be contributing factors. Although recent work described the expression mRNA and protein for the of glucose transporters GluT-1 and in particular GluT-12 in prostate cancer,[86] it is uncertain whether expression levels and activity are in any way related to tumor metabolism or aggressiveness. There also is conflicting data concerning the relationship between FDG uptake in prostate cancer and clinical markers of tumor aggressiveness. At least one study suggested an increased probability for a positive FDG-PET scan in patients with advanced clinical stage and higher PSA (but not Gleason score)[26]; no such relationship was found in another study (whereas tracer uptake in the primary tumor did not correlate with Gleason grade or levels of PSA in other reports.[87]

Efforts have been made to reduce urinary bladder activity from renally excreted FDG, which might cause streak artifacts and interfere with the detection of abnormal FDG uptake in the adjacent prostate gland.[29,87] These efforts included forced diuresis and constant bladder irrigation via an indwelling Foley catheter. These procedures, which are time-consuming and do not seem practical in a busy outpatient PET center, have generally not improved the results. For instance, Effert and coworkers[29] used FDG-PET in 48 patients with various stages of prostate cancer and 16 patients with BPH. Despite continuous bladder irrigation during image acquisition, the authors did not find any difference in intensity or patterns of tracer uptake between cancer and benign prostate hypertrophy. Liu and coworkers[87] used oral hydration and intravenous Lasix for forced diuresis and reported similar results. They included 24 patients with organ-confined newly diagnosed prostate cancer and a mean PSA level of 13 ng/mL (range, 3.7–28.1). All but one patient had a Gleason score of 6 or greater. Histopathology from biopsies or prostatectomy specimens served as standard of reference. Using an arbitrary tumor/back ground ratio >2.5, the authors could only identify one carcinoma, yielding a sensitivity of 4%.

Oyama and coworkers[26] compared the diagnostic yield of ^{11}C-acetate and FDG-PET in a mixed group of 22 patients with primary prostate carcinoma. Five patients subsequently underwent prostatectomy whereas 17 were treated with androgen withdrawal therapy. The sensitivity for localizing the primary tumor was 100% for acetate and 83% for FDG. (This high sensitivity for FDG may have been due to the inclusion of many patients with higher stages of the disease.) The intensity of ^{11}C-acetate uptake in the primary tumor was generally higher than that of FDG uptake, with SUVs ranging from 3.3 to 9.9 as compared with 1.9 to 6.3 for FDG. These results are encouraging, but the study had some methodological shortcomings. Patients with BPH were not included for comparison and histologic proof was only provided for the primary tumor but not sites of suspected metastases. Indeed, several studies have now shown that neither FDG nor acetate or choline reliably distinguish between prostate cancer and benign changes, such as BPH or prostatitis.[28,29,53,65,87] De Jong and coworkers[65] compared uptake patterns of ^{11}C-choline in 25 patients with biopsy proven carcinoma and 5 with BPH. Although all primary tumors were detected and noncancerous prostate tissue, on average, showed lower tumor uptake than did cancer, there was considerable overlap in SUV (SUV_{benign}: mean = 2.3, range 1.3–3.2; SUV_{cancer}: mean = 5.0, range: 2.4–9.5). Using ^{11}C-acetate, Kato and coworkers[53] found no difference in prostate SUV between older subjects with normal prostate (2.3 ± 0.7) and patients with proven prostate cancer (1.9 ± 0.6).

Incidentalomas. Occasionally, focal intense tracer uptake can be noted in the prostate gland. This can be noted for FDG and has also been described for ^{11}C-choline. With the use of combined PET-CT, it is now possible to localize the foci accurately and distinguish them from focal excreted tracer in the prostatic urethra (Fig. 1). Just as for thyroid "incidentalomas," such findings always require further investigation; we recommend at least a digital rectal examination and PSA measurement.

Metastatic Disease

Both nodal and osseous metastases are relatively rare in the current patient population with newly diagnosed prostate carcinoma. For instance, before the widespread use of serum PSA for prostate cancer screening, the number of patients with pelvic lymph node metastases at the time of radical prostatectomy for clinically localized carcinoma was greater than 20%.[88] In more recent series, because most prostate cancers are detected early, this has decreased to 2 to 10%.[89,90] The prevalence of pelvic lymph node metastases correlates directly with T stage, serum PSA levels, and histologic grade.[5] Consequently, a high suspicion of lymph node metastases is based on the finding of 1) prebiopsy serum PSA level greater than 20 ng/mL, 2) poorly differentiated tumor on needle biopsy of the prostate (Gleason score 8-10), or 3) palpable locally advanced tumor.[91] In these patients, the probability for nodal metastases is 30% or greater.[91,92] Detection and localization of metastases is an important clinical issue in this group of patients, which may affect patient management. Once enlarged lymph nodes are detected, CT-guided biopsy can be performed before embarking on prostatectomy or radiation therapy. Treatment with curative intent may not be justified once the cancer has spread to lymph nodes and distant sites. Unfortunately, the statistical nature of nomograms does not provide accurate information in the individual patient.

In addition, whether lymph node metastases are found depends on the extent of the lymphadenectomy.[93,94] Further, it has been

osseous metastases was less than 1% in patients with PSA of <20 ng/mL: among 306 men only 1 (PSA 18.2 ng/mL.) had a positive bone scan, yielding a negative predictive value 99.7%.[109] Others have suggested that bone scans should not be ordered if the PSA is <10ng/mL.[110]

Role of PET

It is generally accepted that FDG-PET has too low a sensitivity to be useful for the diagnosis of lymph node metastases during primary staging of prostate cancer.[30,111] In an initial study of 34 patients with untreated prostate cancer and known or suspected metastases, Shreve and coworkers[30] compared FDG with CT bone scan and clinical follow-up. The evaluation of pelvic lymph nodes was severely limited by bladder activity and streak artifacts. And although the quality of FDG-PET images of the pelvis has improved significantly with the use of iterative reconstruction algorithms, it is unlikely that this test could reliably diagnose nodal metastases in the primary staging. As stated above, many primary prostate cancers show relatively low FDG uptake, and the same is likely also true for nodal metastases.

Similarly, FDG also has a limited sensitivity for the detection of osseous metastases. Shreve and coworkers[30,112] reported a sensitivity of 65% in 22 patients with 202 bone lesions (SUV 2.1–5.7). An even lower detection rate was reported by Yeh and coworkers[112]: only 16% of lesions noted on bone scan were visualized by FDG-PET. However, more recent evidence suggests that FDG is an accurate means in assessing the biologic activity of bone metastases (see the section "Response to Therapy and Prognostic Value").

^{11}C-acetate PET detected lymph node and bone metastases with 100% and 86% sensitivity, respectively.[26] However, both the number of patients studied and number of lesions were very small, so that further investigation is clearly needed.

The utility of ^{11}C-choline PET for nodal staging of prostate cancer before prostatectomy was assessed by de Jong and coworkers.[66] In 67 patients, lymph node metastases were detected with a sensitivity of 80% and specificity of 96%. PET scan was true positive in 12 of 15 patients with histologically proven nodal metastases and was true negative in 50 of 52 without metastases. Of note, a solitary distant nodal metastasis was found in the common iliac nodes in 5 of these 12 patients.

Although PET bone scanning with ^{18}F-fluoride, especially in combination with CT looks extremely promising,[113] it is likely that ^{18}F PET bone scanning will be useful in the same general clinical situation, ie, patients with PSA >20 ng/mL and suspicion for osseous metastases.

PSA Relapse

In most cases, recurrent disease presents initially as biochemical recurrence (BCR), with an increase in serum levels of PSA. Approximately one-third of patients undergoing radical prostatectomy and a similar number of patients with radiation therapy will develop BCR. In the majority of cases, this early rise in PSA occurs in isolation without any symptoms or other objective findings. The clinical behavior of the patient group is extremely heterogeneous and it is not unusual for patients to survive for 5 to 10 years with an elevated PSA as the only evidence of recurrent disease. Imaging studies are frequently negative.

Conventional Imaging Studies

Local Recurrence. The most commonly used imaging technique in the detection of local recurrence is TRUS. The technique is more sensitive than digital rectal examination (75% versus 44%) but less specific (67% versus 91%).[114] In this study the overall TRUS-guided biopsy detection rate was only 41%. The likelihood for tumor detection was higher in patients with a PSA greater than 4 ng/mL. It is difficult to estimate the rate of false-negative TRUS and TRUS-guided biopsies, but as many as 28% of patients with normal initial biopsies demonstrate cancer in subsequent biopsies.[115,116]

CT is not a suitable method for the early detection of local recurrence.[117-119] In nonselected patients, the rate of CT-detected local recurrences was only 11% (2 of 18 patients), despite a relatively high PSA level of 12.4 ng/mL and a mean PSA velocity of 30 ng/mL/yr.[118] In another study only 36% of local recurrences were detected, and in all of these patients the lesion was larger than 2 cm in size.[119] Salvage RT appears most effective in patients with PSA relapse of less than 1.5 ng/mL,[120] and CT cannot detect these early and small recurrences. However, CT can be used for monitoring previously established nodal and visceral disease.

MRI has been investigated for its use in identifying local recurrence and metastatic bony disease in patients with rising PSA after radical treatment.[121-123] In a small number of patients MRI appeared to have a high sensitivity and specificity of 100% for detecting local recurrence after radical prostatectomy.[124] Similar data (sensitivity 95% and specificity 100%) were reported in a recent study in 48 patients with local recurrence.[123] It remains to be seen whether these data can be reproduced outside of specialized centers. Of note, in the latter study 30% of local recurrences were detected outside the prostatic bed (in seminal vesicles, along surgical margins or elsewhere in the pelvis), which would be important for directing biopsies to these sites of suspected disease.

Metastatic Disease. The bone scan is the most commonly used test in patients with BCR; a survey among urologists revealed that 70% order a bone scan a part of the workup in patients with rising PSA after radical prostatectomy or radiation therapy.[125] However, large retrospective studies have shown that the positive yield of a bone scan is less than 1% to 2% in patients with PSA levels less than 10 ng/mL.[110,126,127] Even with PSA levels of 10 ng/mL the fraction of bone scan-detected bone metastases is in the single digit range, and this value is now frequently recommended as the cut-off for ordering a bone scan. In one study the probability for a positive bone scan was less than 5% until PSA increased to 40 to 45 ng/mL. The use of clinical nomograms may help refine the patient population in whom a bone scan should be performed. In patients with abnormal bone scan, the extent of osseous metastatic disease from prostate cancer is an independent prognostic marker.[128-130]

The role of CT in the detection of bone metastases is limited and its routine use not recommended. In contrast, MRI is both sensitive and specific for this purpose. MRI can detect metastases earlier than the bone scan, when they are still developing in the bone marrow. The bone marrow survey is a dedicated MRI technique that covers the axial and proximal appendicular skeleton. The inability to cover the entire skeleton at a reasonable time and at reasonable cost has prevented the widespread use of whole body MRI for detection of metastases. Although newer MRI techniques can cover the entire torso within a reasonable time[131] it is unlikely that the method will enjoy widespread use in patients with prostate cancer.

Lymph node metastases can be detected by CT or MRI but at this time both are limited by their use of size criteria. In a retrospective study in 45 patients, the fraction of CT-detected lymph node metastases was higher in patients with PSA levels of greater than 4 ng/mL (50%) than in those with lower PSA levels (17%).[25]

Contribution of PET

Studies With FDG. Seltzer and coworkers[25] imaged 45 patients with BCR (mean PSA 3.8 ng/mL) with abdominopelvic CT and

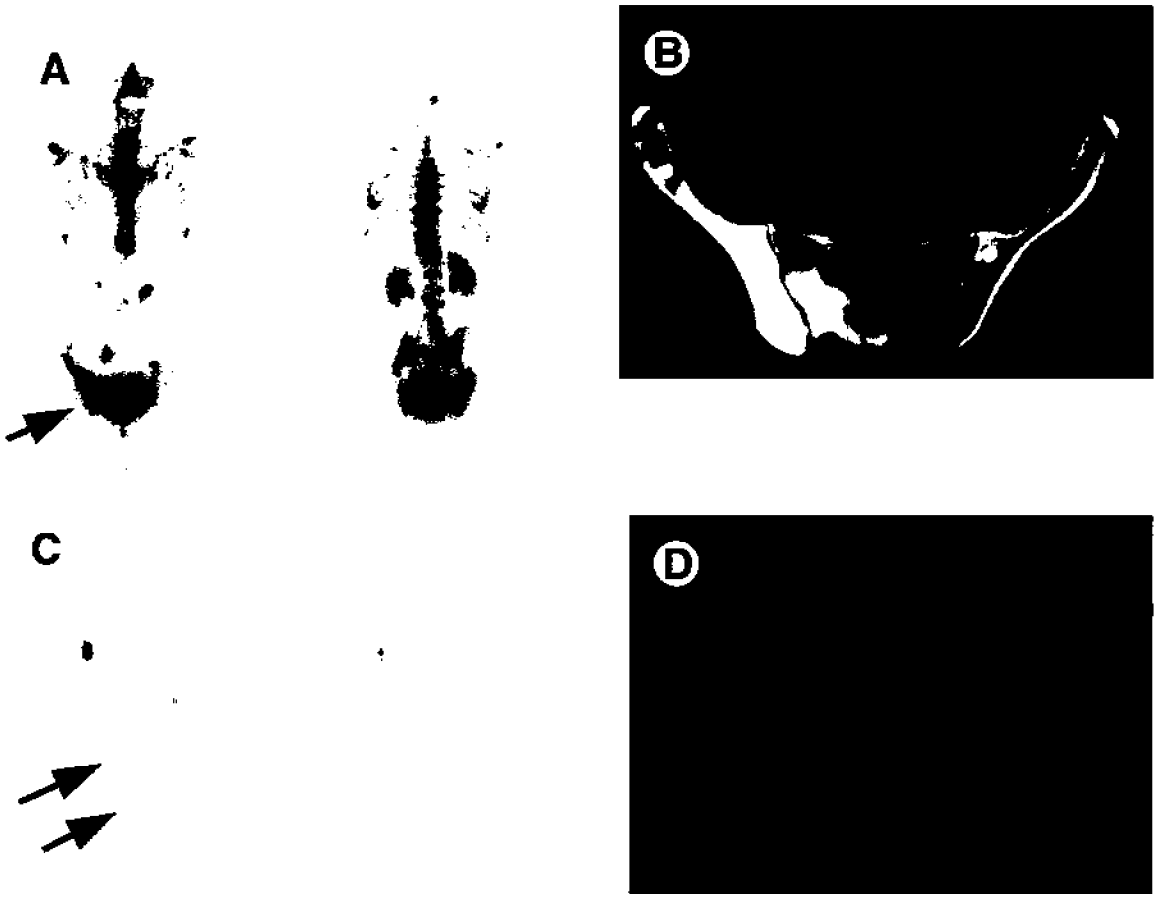

Figure 2 62-year-old male with osseous metastases from prostate cancer; PSA = 6.5 ng/mL. (A) Bone scan shows abnormal tracer uptake in the spine and pelvis. (B) CT, (C) PET, and (D) PET/CT fusion images of the pelvis. Note absence of FDG uptake in the sclerotic lesion in the right iliac bone, which shows intense tracer uptake on the bone scan. (Color version of figure is available online.)

FDG-PET. CT and PET were positive for nodal metastases in 33% and 27%, respectively. The authors then applied an arbitrary cut-off value for PSA and found a higher detection rate for lymph node metastases in patients with PSA greater than 4 ng/mL (CT: 50%, PET: 50%) as compared with those with lower PSA levels. The study had some limitations in that attenuation correction was not routinely performed, biopsy confirmation was available in only 12 of the 45 patients, and a method-inherent bias favored CT results (only enlarged lymph nodes were biopsied). It was concluded that both imaging modalities are of limited use for the detection of metastatic disease in patients with low levels of PSA. In our own experience in 93 patients with BCR and a PSA of 4.38.6 ng/mL, FDG-PET was positive in 35% of cases, detecting local recurrence, nodal, or osseous metastases. The majority of true-positive lesions (30 of 35) were distant metastases (Figs. 2 and 3). A PSA level of 2.4 ng/mL provided the best tradeoff between patients with positive and negative scan (sensitivity/specificity 79%/66%). Because of the low yield of true-positive findings, FDG-PET is therefore not recommended in post-prostatectomy patients with BCR whose PSA levels are less than 2.4 ng/mL.[27]

Other PET tracers, in particular choline and acetate, have been studied in patients with PSA relapse. According to unanimous initial reports these agents hold great promise for detecting recurrent disease in patients with BCR.[38,39,63,67]

Studies With Acetate. The value of ^{11}C-acetate in patients with BCR has been addressed specifically in three studies,[31,38,39] which included a total of approximately 100 patients. Kotzerke and coworkers[39] specifically studied the value of ^{11}C-acetate PET in visualizing local recurrence in the prostate bed and adjacent tissues. Thirty-one patients with BCR and a mean PSA of 15 ± 30 ng/mL (range 0.9–151) were included. TRUS (followed by biopsy if suspicious nodules were detected) and 6 months of clinical follow-up served as standard of reference. Recurrent disease was eventually proven (21 biopsy, 2 TRUS only) in 18 patients. PET showed focal abnormal tracer uptake in the prostate bed in 15 of these individuals (sensitivity 15/18 = 83%). PET was false negative in three patients (PSA 1.3; 4.4 and 12.6 ng/mL). There were no false-positive findings. In addition to local recurrence, distant lymph node or bone metastases were seen in five patients each. The proportion of tumors detected appeared independent of PSA levels. In a subgroup of patients with PSA levels less than 2 ng/mL, five of eight local recurrence were noted by PET, thereby identifying patients who might benefit from salvage RT. (Salvage RT for local recurrence appears most promising in patients with PSA levels <1.5–2.0 ng/mL[132] and would only be initiated in patients without distant disease.) The three tumors not detected by acetate PET were less than 1.5 mL in volume.

Oyama and coworkers studied 46 patients with rising PSA after prostatectomy or primary radiation therapy.[38] All patients underwent PET with ^{11}C-acetate and FDG (furosemide and bladder catheter for the latter). Abnormal tracer uptake, suspicious for recurrent disease, was detected in 59% of acetate studies but only 17% of FDG

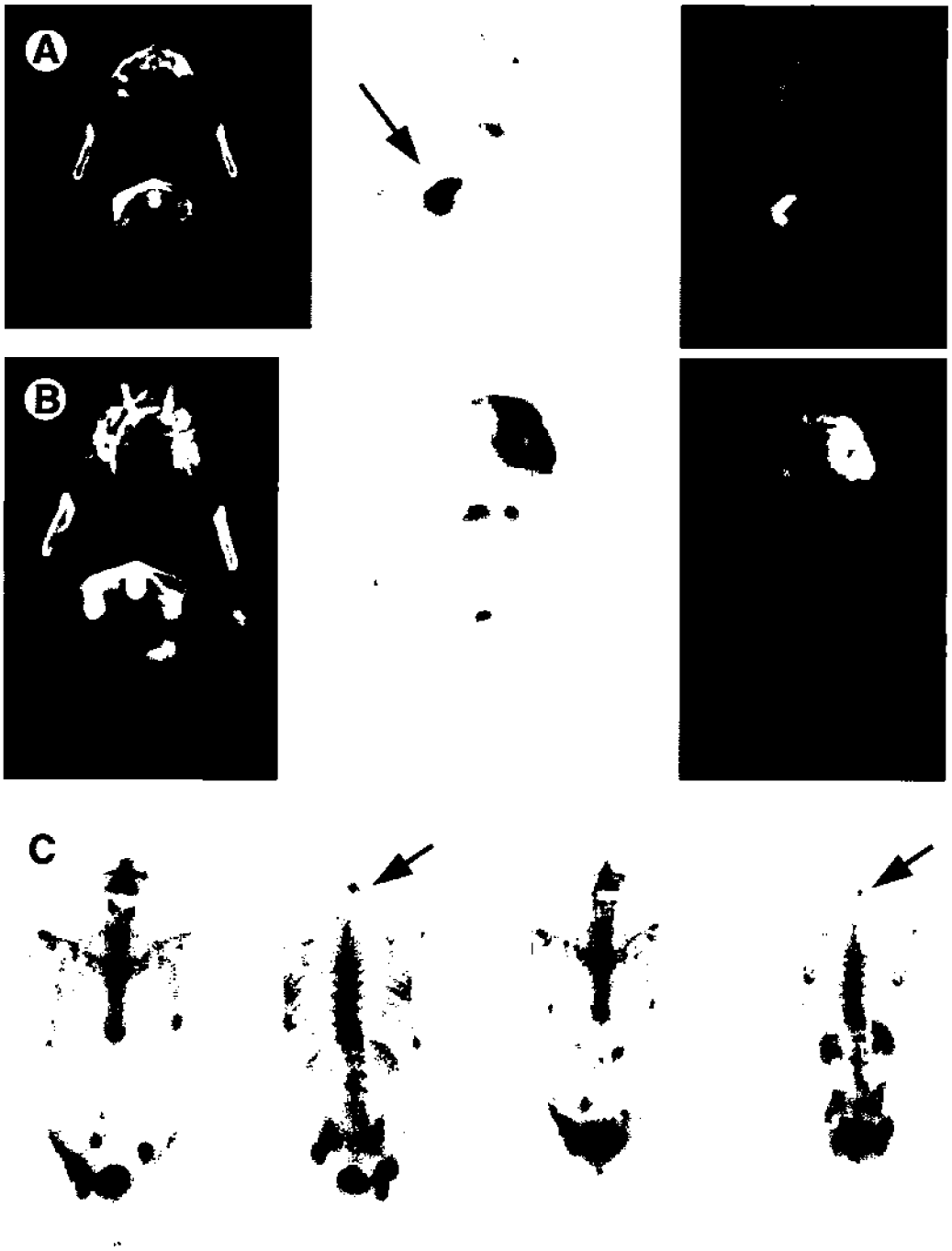

Figure 3 FDG-PET shows response to therapy in this patient with osseus metastases from prostate cancer who had a PSA of 5.88 ng/mL. (A) CT, PET, and PET-CT fusion images show abnormal FDG uptake within a sclerotic lesion in the axis (second cervical vertebra). (B) A follow-up study 6 months later, after combined androgen withdrawal therapy, shows an identical CT image but lack of FDG uptake. (C) Bone scan images at time point 1 (left panel) and 6 months later (right panel) are almost identical with several lesions in spine and pelvis. (Color version of figure is available online.)

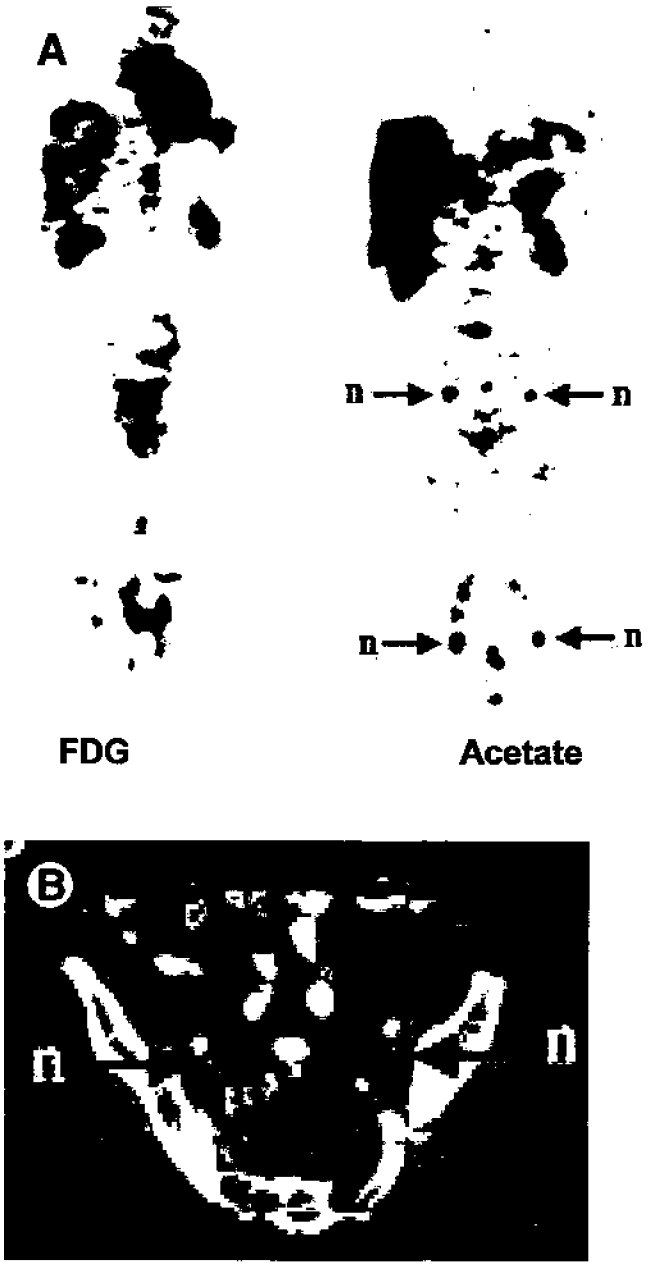

Figure 4 (A) FDG and ^{11}C acetate PET scan in 73-year-old male with PSA relapse (9.1 ng/mL) approximately 2 years after external beam RT with curative intent. FDG images (left panel) show no abnormal tracer uptake, whereas 11C acetate images (right panel) clearly demonstrate abnormal tracer uptake in pelvic lymph nodes. (B) CT shows mildly enlarged pelvis lymph nodes. (Images reprinted by permission of the Society of Nuclear Medicine from Oyama et al.[38]).

studies (Fig. 4). Using CT, bone scan, biopsy, or "high clinical probability" as the standard of reference, 30% of patients had their disease identified by acetate PET, whereas only 9% had disease identified by FDG-PET. In this study, the probability for lesion detection was higher in patients with PSA levels greater than 3 ng/mL (59%) as compared with those with lower PSA levels (4%). This is in contrast to data by Kotzerke and coworkers[39] (see above).

Fricke and coworkers[31] compared FDG and ^{11}C-acetate PET in prostate cancer patients with suspected local recurrence or metastatic disease (PSA range, 0.4–400 ng/mL). An arbitrary SUV greater than 2 was used to identify disease. Overall, local recurrence or metastases were detected in two thirds of patients with FDG and 80% of patients with ^{11}C-acetate. The intensity of FDG uptake in these lesions was generally lower that that for acetate (median SUV 1.4 versus 3.2). In a subset of 15 patients who were imaged with both tracers, acetate showed a higher sensitivity than FDG for local recurrence and nodal metastases (70% versus 43% and 75% versus 30%). However, distant disease mostly in bone) was detected more frequently with FDG (75% of cases versus 50% with acetate). It was suggested that PET imaging with more than one tracer might be necessary in the evaluation of patients with BCR.

Studies With Choline. Price and coworkers[62] investigated the distribution of FDG and F-choline in cell cultures and patients with androgen-dependent and androgen-independent prostate cancer. FCH uptake was 80% and 60% greater than FDG uptake in androgen-dependent and -independent cells. In patients with primary or metastatic prostate cancer, more lesions were visualized with FCH. Prostatic uptake was 2.8-fold higher for FCH than for FDG and appeared more focal. Local disease recurrence was detected in three patients with FCH but only one with FDG. Six patients showed abnormal uptake of FCH in lymph nodes in comparison with two patients with FDG. FCH was retained in tumor tissue for 1 h after administration, consistent with its phosphorylation and incorporation into cellular lipids.

De Jong and coworkers studied 22 patients with rising PSA and 14 without evidence for BCR after prostatectomy or radical radiation therapy[67] ^{11}C-choline PET was true negative in 14 of 14 patients without BCR. Among the 22 patients with elevated PSA levels, sites of recurrent disease were identified in 12 (5 of 13 with radical prostatectomy and 7 of 9 with radiation therapy). In the 10 patients with negative PET, all other imaging studies had also failed to demonstrate sites of disease. Of note, all patients with PSA levels less than 5 ng/mL had a negative PET scan.

The largest study to date was conducted by Picchio and coworkers,[63] who compared ^{11}C-choline and FDG in 100 men with BCR (mean PSA, 6.5 ng/mL; range, 0.14–171). Seventy-seven individuals had undergone prostatectomy, and 23 had been treated with radiation therapy. PET findings were compared with those in "conventional imaging studies" and in those individuals with negative PET using PSA levels after 1 year of follow-up. More abnormalities, suspicious for recurrent disease, were noted with choline than with FDG (47% versus 27% of studies; Fig. 5). Patients (35 of 47) with abnormal choline scan also had recurrent disease identified by conventional imaging. There was only one patient with negative choline scan in whom conventional imaging studies found the site of disease. Overall, choline PET proved more accurate than FDG for detecting local recurrence as well as nodal and distant metastases. A negative choline scan likely indicates a good prognosis because 80% of these patients showed stable PSA levels at 1 year of follow-up.

Studies With Methionine. Nunez and coworkers[34] compared the diagnostic yield of FDG and ^{11}C-methionine in 12 castrate patients with progressing prostate cancer, defined as 50% increase in the PSA levels and the development of new lesions or worsening of preexisting lesions on bone scan, CT, or MRI. Of all lesions assessed, 93% were osseous metastases. On average, the intensity of methionine uptake in these lesions was significantly higher than that of FDG and more lesions were detected with ^{11}C-methionine PET. The number of lesions on methionine PET correlated better with the number of lesions on bone scan. Using conventional imaging (CT, MRI, bone scan) as the their standard,

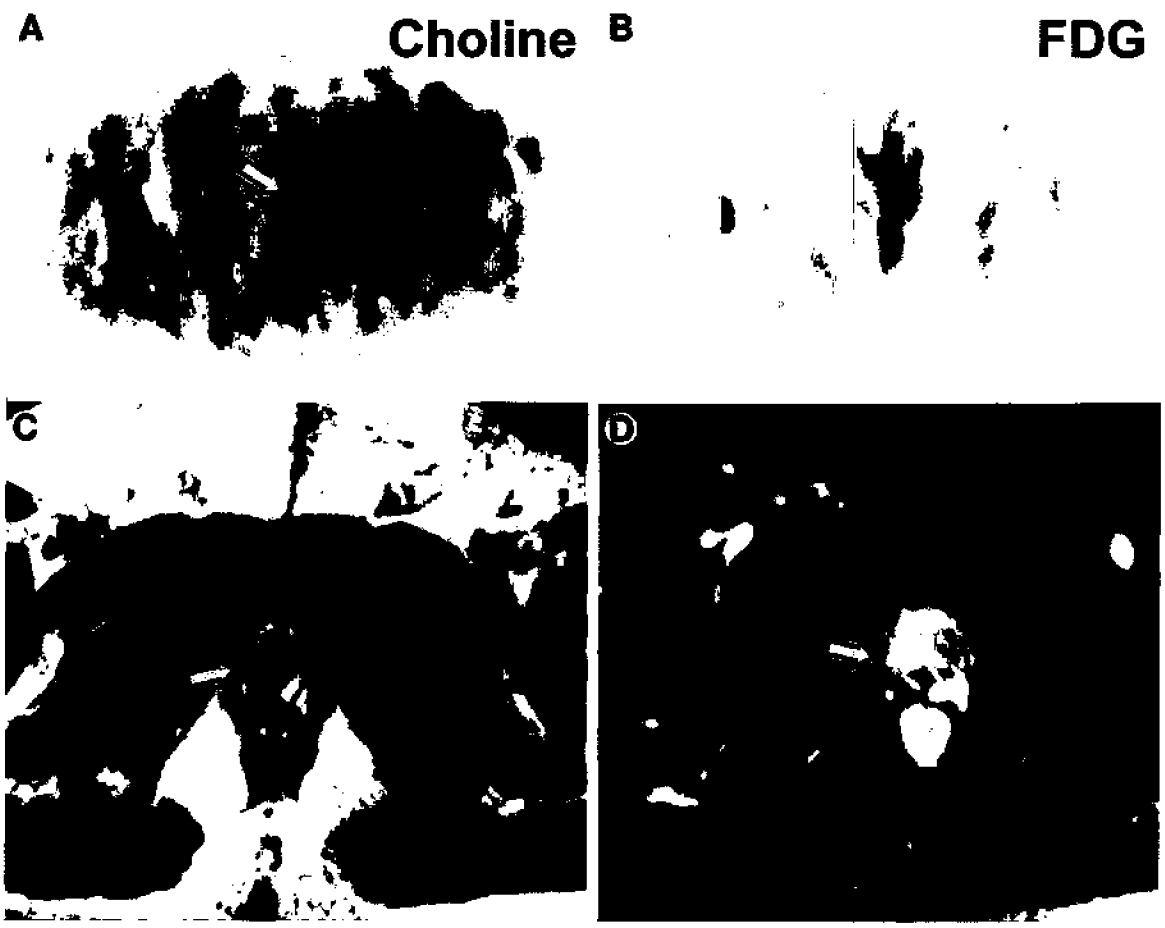

Figure 5 Transaxial PET images in a patient with a man with PSA relapse (PSA = 3.8 ng/mL) approximately 6 years after radical prostatectomy. ^{11}C choline PET shows abnormal tracer accumulation in the prostate bed (A), whereas FDG image appears normal (B). T_2-weighted spine-echo MRI (C) and contrast-enhanced, fat-suppressed T_1-weighted MRI (D) clearly show abnormal soft tissue in the prostate bed (arrows). (Images used with permission from Picchio et al. J Urol 169:1337-1340, 2003.)

the sensitivity for the detection of bone and soft tissue metastases was 48% and 34%, respectively, for FDG-PET as compared with 70% and 70%, respectively, for ^{11}C-methionine PET. The authors speculated that FDG might reflect the biologic activity of the disease more accurately than bone scan or methionine PET.

Response to Therapy and Prognostic Value

Treatment Monitoring

Most prostate cancers are dependent on androgen for growth and metastasis. Therefore, androgen ablation is one of the main treatment modalities in patients who do not qualify for radical treatment with curative intent and also for many patients with recurrent or metastatic disease. In selected cases, chemotherapy is also used.[133,134] The current means of assessing the response to hormonal and chemotherapy are imprecise and inadequate because changes in tumor size are often slow to occur and alterations in PSA levels do not always correlate with clinical outcome.[135,136] For instance, androgen blockade causes a decline in PSA to undetectable levels, but this does not necessarily reflect an improved survival in these patients.[135] Also, bone lesions are notoriously difficult to quantitate on conventional imaging studies, and bone scan may actually get worse, even when tumor has responded ie, ("flare" phenomenon).[137,138]

Experimental and clinical studies (Figs 2 and 3) suggested that PET can monitor the course of prostate cancer and its response to therapy.[24,33,70,139,140] Using a human prostate cancer xenograft model, Agus and coworkers[24] studied serial changes in prostate cancer metabolism with ^3H DOG or FDG-PET. At 48 h after androgen withdrawal, glucose accumulation in the tumor was decreased to 62% of baseline level and decreased further to 32% of baseline after 10 days. Changes in tumor metabolism preceded changes in tumor volume and PSA. The decline in tumor glucose uptake also was associated with a decrease in the proportion of tumor cells in the active cell cycle. Reintroduction of androgen caused a return of glucose uptake to near baseline levels. Similar data were reported by Oyama and coworkers[140] using a tumor-bearing mouse model and micro PET imaging. Treatment with diethylstilbestrol, simulating androgen withdrawal therapy, caused a decrease in FDG uptake in the prostate at 3 weeks. No such change was noted in control animals or those treated with dihydrotestosterone. These experimental studies and preliminary data in patients suggested that FDG-PET could be used for treatment monitoring in prostate cancer patients. In a small series of 10 patients, Oyama and coworkers[139] used FDG for monitoring the response to androgen ablation therapy. PET was performed before and then again between 1 and 5 months after initiation of hormonal therapy. All patients showed a decrease in

PSA levels as well as FDG SUV in the prostate gland and at metastatic sites. PSA levels declined by 70% to 99% compared with baseline and the SUV decreased by 12% to 77% compared with baseline. Of note, there was no correlation between these two parameters. Although these findings suggested that glucose use in human prostate cancer is suppressed by androgen ablation, it remains to be seen if and how the data can be used to guide patient management. In a mouse model, the proliferation marker F-18 FLT also appeared to be suitable for monitoring the response of to androgen withdrawal therapy.[141]

Using F-18 choline as a PET tracer, DeGrado and coworkers[70] describe the response to androgen withdrawal therapy in a patient with metastatic prostate cancer. Although the lesion was still visualized on the follow-up scan, the intensity of choline uptake had decreased significantly (approximately 60% decline in SUV as compared with baseline).

As stated above, FDG-PET detects fewer osseous lesions than either bone scan or CT.[30,112] However, these two imaging modalities only reflect abnormal osteoblast activity or structural alterations in the bone, which do not necessarily indicate the presence of viable tumor cells. Abnormalities on bone scan can persist for many years, although no viable tumor can be found on biopsy. As mentioned above, an increase in tracer uptake in the bone scan after therapy can reflect treatment-induced changes in blood flow and osteoblast activity rather than an increase in tumor burden ("flare phenomenon"). In patients that show a flare phenomenon on bone scan, FDG-PET may reflect more accurately the response to therapy.[142]

Prognostic Value

For a number of malignancies, the intensity of tracer uptake can serve as an independent indicator of the patient's prognosis both in the primary setting as well as for recurrent disease.[143-145] Limited evidence suggests that this also may apply in patients with prostate cancer[146]: among surgically treated patients, those with low FDG uptake in the primary tumor (SUV <4) appeared to have better relapse-free survival. However, the same authors also reported[26] that the probability for a positive PET scan in patients with newly diagnosed prostate cancer increases with advancing stage as well as increases in PSA levels, which are established prognostic factors.[11] Therefore, it remains to be seen whether PET provides truly independent prognostic information in prostate cancer.

The prognostic value of FDG-PET in patients with bone metastases was addressed in a study by Morris and coworkers.[33] Of a total of 137 of the lesions (in 17 patients), 71% were noted on both PET and bone scan, whereas 23% were only seen on bone scan and 6% only on PET. Of note, all but one of the lesions noted on bone scan alone remained stable, but al lesions detected only by FDG-PET showed further progression with positive bone scans developing at the site on follow-up. This suggested that FDG-PET might reflect more accurately the tumor biology and aggressiveness of the disease.

Conclusions

The usefulness of PET is strongly influenced by the clinical state and aggressiveness of the individual patient's tumor. This fact has been given insufficient weight in many early studies of the role of PET in prostate cancer, and clinical status is often incompletely reported. This makes interpretation of the findings of individual studies problematic. Nevertheless, it is clear that for many patients with primary prostate cancer, PET is not a useful test for initial detection. However, from a practical point of view, this may be less relevant. In most men now being diagnosed with prostate cancer, workup is initiated because of an incidentally detected elevated PSA level during routine physical examination. Further evaluation almost always includes consultation with an urologist, digital rectal examination, transrectal ultrasound and (TRUS-guided) biopsy of the prostate. Because this diagnostic paradigm is now widely accepted, few of the more recent imaging studies have attempted to diagnose prostate cancer or distinguish it from BPH.

With regard to staging, neither CT nor MRI, as currently practiced, reliably detect lymph node metastases from primary prostate carcinoma. A bone scan should only be ordered in selected patients, based on significant elevation (>20 ng/mL) of the PSA. PET with FDG is not helpful in detecting nodal metastases in the primary setting. ^{11}C-acetate or choline appear more promising for identifying metastatic disease, but their exact role in the management of patients with primary prostate cancer requires further investigation.

FDG-PET can identify recurrent disease, nodal, and osseous metastases in patients with PSA relapse. Lower thresholds for PSA have been identified, above which FDG is more likely to detect disease. Similar thresholds likely also exist for imaging with acetate or choline.[38,67] Neither acetate nor choline is the "perfect" radiotracer, and local recurrence or small nodal metastases can be missed. Nevertheless, PET with choline or acetate generally shows more sites of disease and more intense uptake in these lesions than FDG. One study suggested that imaging with 2 tracers may be required in patients with PSA relapse, because local recurrence and lymph node metastases were detected better with acetate, but bone lesions better with FDG.[31]

Renal Cell Carcinoma (RCC)

RCC accounts for approximately 3% of all cancers in adults, and approximately 36,000 cases will be diagnosed in 2004 in the United States.[1] With the increased use of ultrasound and CT for the evaluation of abdominal diseased, the number of incidentally discovered RCCs has increased significantly.[147] Surgery is the only definite form of therapy in these patients. Curative resection is feasible for localized disease (including stages I, III, IIIa) and the prognosis after resection of the primary tumor is good.[147] However, the prognosis is bleak in patients with overt metastases at the time of diagnosis, with a median survival of 10 months.

CT is the standard imaging test for evaluation of patients with renal masses.[148] Helical CT may identify RCC with a sensitivity of 100% and specificity of 88% to 95%.[149,150] The reported sensitivity of CT for the detection of retroperitoneal lymph node metastases is as high as 95%,[148] but using a nodal size of 1 cm or greater as criterion, the rate of false-positive findings can range from 3% to 43%.[151] Despite recent advances in CT technology, the sensitivity for the detection of pulmonary metastases from extra-thoracic primary tumors ranges from 75% to 95% but is lower (50-70%) for lesions smaller than 6 mm in size.[152,153]

Detection of Primary Disease

Few studies have investigated the utility of PET in the assessment of renal masses and primary staging of RCC. In a pilot study in five patients with RCC, all primary tumor and metastases were visualized by FDG-PET.[154] This prompted further investigations in patients with primary RCC as well as those with suspected local recurrence or metastatic disease. In a study of 29 patients, PET was positive in 20 of 26 with confirmed disease, but the primary tumor was missed in 6 cases. An angiomyolipoma, a pericytoma, and a pheochromocytoma showed a false-positive PET result.[155] In a more recent study[156] a primary RCC was identified in 15 of 17 patients with suspicious renal masses. There were no false-positive results.

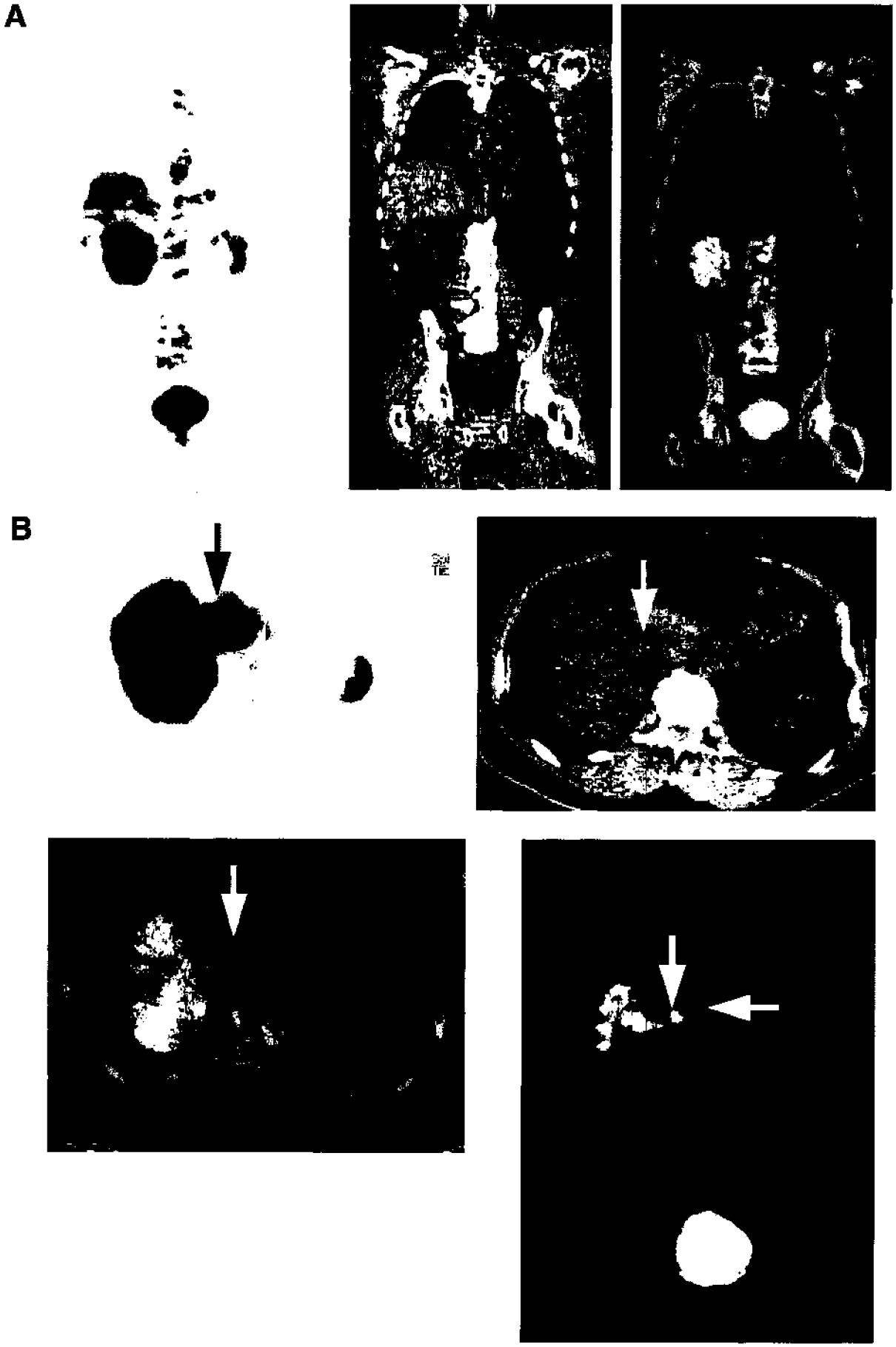

Figure 6 Staging of RCC. (A) Coronal FDG-PET images, coronal CT, and coronal PET/CT fusion images show abnormal FDG uptake in a right renal mass. (B) Transaxial PET, CT, and fusion images, as well as coronal PET-CT fusion image, show tumor extension into the right renal vein and inferior vena cava. (Color version of figure is available online.)

Overall, PET influenced treatment decisions in 6 of 17 patients (35%); 2 were found to have metastases by PET, whereas renal vein thrombus was excluded in 1, and 3 were considered eligible for nephron-sparing surgery. The overall accuracy was 94%, which was identical to CT in this study. However, this high sensitivity of PET could not be reproduced in other studies.[157,158] In the largest study to date, Kang and coworkers[157] performed FDG-PET in 66 patients with RCC. Of the 17 individuals with known primary RCC or suspicious mass, 15 were found to have a primary renal cancer; only 9 of these tumors appeared hypermetabolic on FDG-PET and were thus correctly classified as cancer. The PET sensitivity and specificity for the detection of primary RCC were 60% and 100% (CT: 92% and 100%). An image example is shown in Figure 6.

Recurrent and Metastatic Disease

Metastatic disease is a strong predictor of poor survival in patients with RCC.[159] Patients with advanced metastatic disease have a 0% to 2% 5-year survival rate,[160] whereas solitary metastases can be resected surgically in selected patients, with a 5-year survival rate of approximately 30%.[161] Early detection and management of metastases has the potential to improve prognosis and quality of life. Currently CT, sometimes supplemented by a bone scan if indicated, is the most commonly used imaging test for follow-up of patients with RCC. Although FDG-PET did not appear to contribute much to the initial staging of RCC, the detection of local recurrence or metastases should not be affected by some of the FDG-inherent limitations in imaging the urinary tract.[156,157,162-165]

The aforementioned study by Ramdave et al[156] included eight patients with suspected local recurrence or metastatic disease. PET was true positive in seven patients and true negative in one, yielding a diagnostic accuracy of 100% (CT: 88%). Of eight patients in whom CT suggested potentially resectable metastatic disease, PET revealed widespread metastases in four. In one patient, PET accurately distinguished between postradiation changes and local recurrence. The findings lead to a change in treatment in four of eight patients (50%) by avoiding or altering planned surgical procedures.

Safaei and coworkers[164] performed PET in 36 patients with advanced renal cell cancer who were referred for restaging. 85% of confirmed lesions were assessed accurately (sensitivity 88%, specificity 75%). They concluded that PET could be useful in characterizing anatomic lesions of unknown significance.

Majhail and coworkers[165] studied 24 patients with RCC and suspected recurrence at distant sites. Of the 33 sites of histologically proven metastatic sites, 21 (64%) were identified by PET. Sensitivity and specificity were 64% and 100%. These findings were independent of initial Fuhrman grade, prior immuno- or chemotherapy, or the site of distant metastases. However, the average size of metastatic lesions correctly identified by PET was larger than that for false-negative findings (2.2 cm versus 1.0 cm; $P < 0.01$). In no case did FDG-PET identify distant metastases that had not been visualized by CT or MRI.

In the larger study by Kang and coworkers,[157] a total of 172 soft tissue and bone lesions were confirmed as metastatic RCC either by subsequent imaging studies or histopathology, and 115 of these (67%) were identified by PET. Specifically PET detected 89 of 139 soft tissue metastases (64%) and 26 of 33 bone metastases (78%). Lung metastases were detected with a sensitivity of 75% and specificity of 97%. As expected, CT was more sensitive than PET in detecting lung metastases (91%). In addition, the combination of CT and bone scan showed higher sensitivity for detecting osseous metastases (94%). For retroperitoneal nodal metastases, PET was 75% sensitive and 100% specific (CT: 93% and 98%). Multiple lesions within a single patient often exhibited differing levels of FDG uptake and some were undetectable: In 44% of studies PET detected all metastatic lesions, in another 44% only some lesions, and in 12% PET failed to detect any metastasis. Overall, the specificity of PET was generally higher than that of any other test or a combination of CT and bone scan (for bone lesions). In 39 scans (in 32 pats) PET failed to detect RCC lesions identified by conventional imaging.

Conclusion

CT, not PET, is the method of choice for the detection and staging of primary RCC. FDG-PET has a limited sensitivity for evaluating metastatic RCC, in particular for small metastatic lesions. Although a negative study cannot rule out metastatic disease with sufficient accuracy, a positive PET scan should be considered strongly suspicious for local recurrence or metastasis, because of the high specificity and PPV of this test. However, because of the limited anatomic information, PET cannot replace the need for CT in the follow-up of RCC patients. A combined test (CT and PET) may be necessary if important management decisions were to be based on the test result. This would take advantage of the high sensitivity of CT and high specificity of PET in patients with metastatic RCC. PET can also serve as a "problem-solving" modality in cases with equivocal CT or bone scan findings and may prove useful in monitoring treatment response as more effective treatments become available.

Bladder Cancer

Bladder cancer is the fourth most common malignancy in men in the United States, and approximately 60,000 new cases are expected to occur in 2004.[1] Most of the newly diagnosed tumors are low grade and noninvasive. They recur frequently but rarely progress to muscle invasive or metastatic disease. It is unlikely that PET imaging could contribute to the management of these tumors. In contrast, high-grade or invasive bladder cancer is characterized by progressive local invasion, extension to adjacent organs, and the development of regional and distant metastases. Radical cystectomy with pelvic lymphadenectomy is the standard of treatment for patients with invasive disease that is confined to the pelvis. The effectiveness of local therapy depends largely on the extent of primary tumor invasion and the presence of pelvic lymph node metastases: Organ-confined bladder cancer can be treated by surgery alone and may be curable in more than 70% of patients,[166-168] but patients with regional nodal metastases show a propensity for disease recurrence and distant disease and, as a group, show a 5-year survival of only 20% to 25% patients.[166-169] Accurate staging of bladder cancer is therefore important to select the appropriate treatment strategy. Advances in surgical techniques for cystectomy and pelvic reconstruction have made it possible to tailor surgery to the specific needs of patients. Preoperative knowledge of local tumor extension would help in selecting appropriate patients for bladder sparing surgery, nerve or vaginal sparing procedures or pelvic exenteration. Historically, the accuracy of CT for the staging of bladder cancer has been as low as 50% as compared with approximately 75% with MRI.[170-173] The introduction of multi-detector row CT, new MR techniques and MR contrast agents could potentially improve the staging accuracy. Nevertheless, anatomic imaging techniques have method-inherent limitations for the assessment of lymph node metastases as well as for the detection of local recurrence.

Scant work has been done with PET in bladder cancer.[111,155,174] Renal excretion of FDG and streak artifacts from excreted tracer in the urinary bladder led many investigators to conclude that PET would be of limited value in bladder cancer. Although efforts have

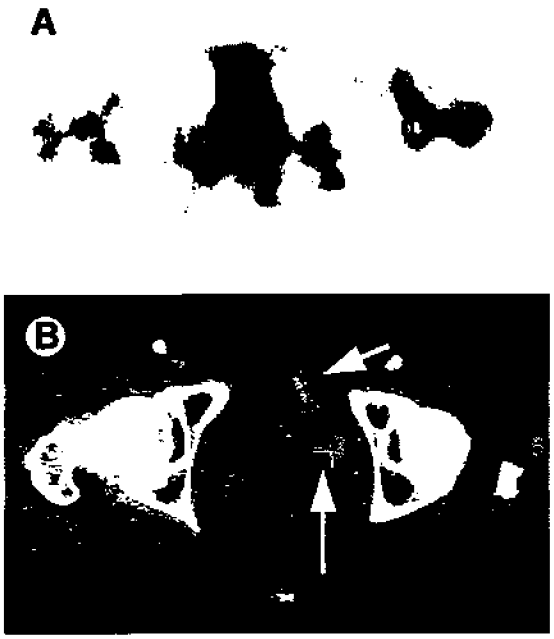

Figure 7 Bladder cancer imaging with FDG. (A) Transaxial FDG-PET image shows excreted tracer in the urinary bladder. (B) The corresponding CT image shows thickening of the bladder wall and a 1.7 × 1.3 cm left perivesical lymph node, likely metastatic. On PET, however, the tumor cannot be identified because of accumulation of excreted tracer in the bladder. FDG is not a suitable tracer for the staging of bladder cancer.

been made to reduce the amount of excreted FDG in the bladder (forced diuresis, bladder catheter with continuous irrigation), the results have largely been disappointing. Pooling of excreted tracer in the ureters and variable bowl activity presented further challenges (Fig 7). One small study reported a sensitivity and specificity of 67% and 85% in patients with carcinoma of the bladder neck, which was better than CT-MRI.[155] However, because of the above limitations the use of FDG-PET for staging of bladder cancer has not found acceptance in clinical practice. In contrast, based on our experience and sporadic case reports,[175] PET with FDG can be a useful test for the detection of recurrent tumor in the pelvis, differentiation between local recurrent disease versus. postsurgical or postirradiation fibrosis or necrosis and for the detection of distant metastases. The use of combined PET-CT imaging is expected to reduce the number of false-positive findings in the lower abdomen and pelvis, which should increase the accuracy of the test.[176,177] Nevertheless, there is a need to study the efficacy of other PET tracers, without or only limited renal excretion, in bladder cancer. ^{11}C methionine and choline have been proposed for this purpose. With methionine, tracer uptake in the primary tumor was related to tumor grade.[178] However, only 78% of all bladder cancers could be visualized, and PET did not improve the local staging of the disease. de Jong and coworkers performed PET with ^{11}C-choline in 18 patients before cystectomy (but after transurethral resection or biopsy) and in 5 volunteers.[174] Normal bladder tissue showed little tracer uptake and there was only minimal urinary activity. The primary tumor was visualized in 10 patients with residual invasive disease in the cystectomy specimen (mean SUV, 4.7 ± 3.6, range, 1.5–13.0). In another seven patients no residual tumor was found at the time of cystectomy. Premalignant lesions (CIS, dysplasia) were present in three of these but were missed by PET. In the remaining patient PET was true negative. One patient showed unexpected abundant urinary activity that interfered with tumor detection, and one false positive finding was related to inflammatory changes from an indwelling bladder catheter.

Conclusion

Because of its renal excretion, FDG is not a suitable tracer for detecting a tumor in the bladder wall. Its accuracy of FDG-PET for finding lymph node metastases is rather low and the method has not found acceptance for the presurgical staging of bladder cancer. However, recurrent disease in the pelvis can be identified with FDG. For proper interpretation of these studies the reader needs to be familiar with various techniques of bladder reconstruction. The role of ^{11}C-acetate and choline in bladder cancer is under investigation.

References

1. Jemal A, Tiwari RC, Murray T, et al: Cancer statistics, 2004. CA Cancer J Clin 54:8-29, 2004
2. Craft N, Chhor C, Tran C, et al: Evidence for clonal outgrowth of androgen-independent prostate cancer cells from androgen-dependent tumors through a two-step process. Cancer Res 59:5030-5036, 1999
3. Chen CD, Welsbie DS, Tran C, et al: Molecular determinants of resistance to antiandrogen therapy. Nat Med 10:33-39, 2004
4. Scher HI, Heller G: Clinical states in prostate cancer: toward a dynamic model of disease progression. Urology 55:323-327, 2000
5. Partin AW, Kattan MW, Subong EN, et al: Combination of prostate-specific antigen, clinical stage, and Gleason score to predict pathological stage of localized prostate cancer. A multi-institutional update. JAMA 277:1445-1451, 1997
6. Blute ML, Bergstralh EJ, Partin AW, et al: Validation of Partin tables for predicting pathological stage of clinically localized prostate cancer. J Urol 164:1591-1595, 2000
7. Graefen M, Karakiewicz PI, Cagiannos I, et al: A validation of two preoperative nomograms predicting recurrence following radical prostatectomy in a cohort of European men. Urol Oncol 7:141-146, 2002
8. Gleason D: Histological grading and clinical staging of prostatic carcinoma, in Tannenbaum T (eds): Urologic Pathology: The Prostate. Philadelphia, PA, Lea & Febiger, 1977, pp 171-197
9. Kattan MW, Wheeler TM, Scardino PT: Postoperative nomogram for disease recurrence after radical prostatectomy for prostate cancer. J Clin Oncol 17:1499-1507, 1999
10. D'Amico AV, Whittington R, Schnall M, et al: The impact of the inclusion of endorectal coil magnetic resonance imaging in a multivariate analysis to predict clinically unsuspected extraprostatic cancer. Cancer 75:2368-2372, 1995
11. Kattan MW, Eastham JA, Stapleton AM, et al: A preoperative nomogram for disease recurrence following radical prostatectomy for prostate cancer. J Natl Cancer Inst 90:766-771, 1998
12. Rifkin MD, Zerhouni EA, Gatsonis CA, et al: Comparison of magnetic resonance imaging and ultrasonography in staging early prostate cancer. Results of a multi-institutional cooperative trial. N Engl J Med 323:621-626, 1990
13. Smith JA Jr, Scardino PT, Resnick MI, et al: Transrectal ultrasound versus digital rectal examination for the staging of carcinoma of the prostate: results of a prospective, multi-institutional trial. J Urol 157: 902-906, 1997
14. Hricak H, Dooms GC, Jeffrey RB, et al: Prostatic carcinoma: staging by clinical assessment, CT, and MR imaging. Radiology 162:331-336, 1987
15. Yu KK, Hricak H: Imaging prostate cancer. Radiol Clin North Am 38:59-85, 2000
16. Yu KK, Hricak H, Alagappan R, et al: Detection of extracapsular extension of prostate carcinoma with endorectal and phased-array coil MR imaging: multivariate feature analysis. Radiology 202:697-702, 1997

glucose: a novel method of preoperative lymph node staging. Cancer 86:1638-1648, 1999
62. Price DT, Coleman RE, Liao RP, et al: Comparison of [18 F]fluorocholine and [18 F]fluorodeoxyglucose for positron emission tomography of androgen dependent and androgen independent prostate cancer. J Urol 168:273-280, 2002
63. Picchio M, Messa C, Landoni C, et al: Value of [11C]choline-positron emission tomography for re-staging prostate cancer: a comparison with [18F]fluorodeoxyglucose-positron emission tomography. J Urol 169:1337-1340, 2003
64. Kotzerke J, Prang J, Neumaier B, et al: Experience with carbon-11 choline positron emission tomography in prostate carcinoma. Eur J Nucl Med 27:1415-1419, 2000
65. de Jong IJ, Pruim J, Elsinga PH, et al: Visualization of prostate cancer with 11C-choline positron emission tomography. Eur Urol 42:18-23, 2002
66. de Jong IJ, Pruim J, Elsinga PH, et al: Preoperative staging of pelvic lymph nodes in prostate cancer by (11)C-choline PET. J Nucl Med 44:331-335, 2003
67. de Jong IJ, Pruim J, Elsinga PH, et al: 11C-choline positron emission tomography for the evaluation after treatment of localized prostate cancer. Eur Urol 44:32-38, 2003; discussion 38-39
68. Roivainen A, Forsback S, Gronroos T, et al: Blood metabolism of [methyl-11C]choline; implications for in vivo imaging with positron emission tomography. Eur J Nucl Med 27:25-32, 2000
69. Hara T, Kosaka N, Kishi H: Development of (18)F-fluoroethylcholine for cancer imaging with PET: synthesis, biochemistry, and prostate cancer imaging. J Nucl Med 43:187-199, 2002
70. DeGrado TR, Coleman RE, Wang S, et al: Synthesis and evaluation of 18F-labeled choline as an oncologic tracer for positron emission tomography: initial findings in prostate cancer. Cancer Res 61:110-117, 2001
71. DeGrado TR, Baldwin SW, Wang S, et al: Synthesis and evaluation of (18)F-labeled choline analogs as oncologic PET tracers. J Nucl Med 42:1805-1814, 2001
72. DeGrado TR, Reiman RE, Price DT, et al: Pharmacokinetics and radiation dosimetry of 18F-fluorocholine. J Nucl Med 43:92-96, 2002
73. Sutinen E, Nurmi M, Roivainen A, et al: Kinetics of [(11)C]choline uptake in prostate cancer: a PET study [correction for stydy]. Eur J Nucl Med Mol Imaging 31:317-324, 2004
74. Wyss MT, Weber B, Honer M, et al: 18F-choline in experimental soft tissue infection assessed with autoradiography and high-resolution PET. Eur J Nucl Med Mol Imaging 31:312-316, 2004
75. Miyazawa H, Arai T, Iio M, et al: PET imaging of non-small-cell lung carcinoma with carbon-11-methionine: relationship between radioactivity uptake and flow-cytometric parameters. J Nucl Med 34:1886-1891, 1993
76. Lindholm P, Leskinen S, Lapela M: Carbon-11-methionine uptake in squamous cell head and neck cancer. J Nucl Med 39:1393-1397, 1998
77. Lindholm P, Leskinen S, Nagren K, et al: Carbon-11-methionine PET imaging of malignant melanoma. J Nucl Med 36:1806-1810, 1995
78. Ogawa T, Shishido F, Kanno I, et al: Cerebral glioma: Evaluation with methionine PET. Radiology 186:45-53, 1993
79. Schober O, Duben C, Meyer G, et al: Nonselective transport of [11C-methyl]-L- and D-methionine into a malignant glioma. Eur J Nucl Med 13:103-105, 1987
80. Hatazawa J, Ishiwata K, Itoh M, et al: Quantitative evaluation of L-[methyl]-11C methionine uptake in tumor using positron emission tomography. J Nucl Med 30:1809-1813, 1989
81. Kubota R, Kubota K, Yamada S, et al: Methionine uptake by tumor tissue: A microautoradiographic comparison with FDG. J Nucl Med 36:484-492, 1995
82. Nilsson S, Kalkner K, Ginman C, et al: C-11 methionine positron emission tomography in the management of prostatic carcinoma. Antibody Immunconj Radiopharm 8:23, 1995
83. Macapinlac HA, Humm JL, Akhurst T, et al: Differential metabolism and pharmacokinetics of L-[1-(11)C]-methionine and 2-[(18)F] fluoro-2-deoxy-D-glucose (FDG) in androgen independent prostate cancer. Clin Positron Imaging 2:173-181, 1999
84. Craft N, Sawyers CL: Mechanistic concepts in androgen-dependence of prostate cancer. Cancer Metastasis Rev 17:421-427, 1998
85. Bonasera TA, O'Neil JP, Xu M, et al: Preclinical evaluation of fluorine-18-labeled androgen receptor ligands in baboons. J Nucl Med 37: 1009-1015, 1996
86. Chandler JD, Williams ED, Slavin JL, et al: Expression and localization of GLUT1 and GLUT12 in prostate carcinoma. Cancer 97:2035-2042, 2003
87. Liu IJ, Zafar MB, Lai YH, et al: Fluorodeoxyglucose positron emission tomography studies in diagnosis and staging of clinically organ-confined prostate cancer. Urology 57:108-111, 2001
88. Smith JA Jr, Seaman JP, Gleidman JB, et al: Pelvic lymph node metastasis from prostatic cancer: influence of tumor grade and stage in 452 consecutive patients. J Urol 130:290-292, 1983
89. Bundrick WS, Culkin DJ, Mata JA, et al: Evaluation of the current incidence of nodal metastasis from prostate cancer. J Surg Oncol 52: 269-271, 1993
90. Danella JF, deKernion JB, Smith RB, et al: The contemporary incidence of lymph node metastases in prostate cancer: implications for laparoscopic lymph node dissection. J Urol 149:1488-1491, 1993
91. Eastham J, Scardino P: Radical Prostatectomy, in Campbell's Urology. Philadelphia, PA, Saunders, 1998, pp 2547-2561
92. Ohori M, Wheeler TM, Dunn JK, et al: The pathological features and prognosis of prostate cancer detectable with current diagnostic tests. J Urol 152:1714-1720, 1994
93. Bader P, Burkhard FC, Markwalder R, et al: Is a limited lymph node dissection an adequate staging procedure for prostate cancer? J Urol 168:514-518, 2002; discussion 518
94. Heidenreich A, Varga Z, Von Knobloch R: Extended pelvic lymphadenectomy in patients undergoing radical prostatectomy: high incidence of lymph node metastasis. J Urol 167:1681-1686, 2002
95. Edelstein RA, Zietman AL, de las Morenas A, et al: Implications of prostate micrometastases in pelvic lymph nodes: An archival tissue study. Urology 47:370-375, 1996
96. Cheng L, Zincke H, Blute ML, et al: Risk of prostate carcinoma death in patients with lymph node metastasis. Cancer 91:66-73, 2001
97. Zincke H, Lau W, Bergstralh E, et al: Role of early adjuvant hormonal therapy after radical prostatectomy for prostate cancer. J Urol 166: 2208-2215, 2001
98. Graefen M, Karakiewicz PI, Cagiannos I, et al: Validation study of the accuracy of a postoperative nomogram for recurrence after radical prostatectomy for localized prostate cancer. J Clin Oncol 20:951-956, 2002
99. Cheng L, Bergstralh EJ, Cheville JC, et al: Cancer volume of lymph node metastasis predicts progression in prostate cancer. Am J Surg Pathol 22:1491-1500, 1998
100. Steinberg GD, Epstein JI, Piantadosi S, et al: Management of stage D1 adenocarcinoma of the prostate: the Johns Hopkins experience 1974 to 1987. J Urol 144:1425-1432, 1990
101. Seay TM, Blute ML, Zincke H: Long-term outcome in patients with pTxN+ adenocarcinoma of prostate treated with radical prostatectomy and early androgen ablation. J Urol 159:357-364, 1998
102. Oyen R, van Poppel F, van de Voorde W, et al: Lymph node staging of localized prostatic carcinoma with CT and CT-guided fine-needle aspiration biopsy: Prospective study of 285 patients. Radiology 190: 315-322, 1994
103. Wolf JS Jr, Cher M, Dall'era M, et al: The use and accuracy of cross-sectional imaging and fine needle aspiration cytology for detection of pelvic lymph node metastases before radical prostatectomy. J Urol 153:993-999, 1995
104. Tiguert R, Gheiler EL, Tefilli MV, et al: Lymph node size does not correlate with the presence of prostate cancer metastasis. Urology 53:367-371, 1999
105. Flanigan RC, McKay TC, Olson M, et al: Limited efficacy of preoperative computed tomographic scanning for the evaluation of lymph node metastasis in patients before radical prostatectomy. Urology 48: 428-432, 1996

106. Harisinghani MG, Barentsz J, Hahn PF, et al: Noninvasive detection of clinically occult lymph-node metastases in prostate cancer. N Engl J Med 348:2491-2499, 2003
107. Takashima H, Egawa M, Imao T, et al: Validity of sentinel lymph node concept for patients with prostate cancer. J Urol 171:2268-2271, 2004
108. Wawroschek F, Vogt H, Wengenmair H, et al: Prostate lymphoscintigraphy and radio-guided surgery for sentinel lymph node identification in prostate cancer. Technique and results of the first 350 cases. Urol Int 70:303-310, 2003
109. Chybowski FM, Keller JJ, Bergstralh EJ, et al: Predicting radionuclide bone scan findings in patients with newly diagnosed, untreated prostate cancer: prostate specific antigen is superior to all other clinical parameters. J Urol 145:313-318, 1991
110. Lee CT, Oesterling JE: Using prostate-specific antigen to eliminate the staging radionuclide bone scan. Urol Clin North Am 24:389-394, 1997
111. Heicappell R, Muller-Mattheis V, Reinhardt M, et al: Staging of pelvic lymph nodes in neoplasms of the bladder and prostate by positron emission tomography with 2-[(18)F]-2-deoxy-D-glucose. Eur Urol 36:582-587, 1999
112. Yeh SD, Imbriaco M, Larson SM, et al: Detection of bony metastases of androgen-independent prostate cancer by PET-FDG. Nucl Med Biol 23:693-697, 1996
113. Even-Sapir E, Metser U, Flusser G, et al: Assessment of malignant skeletal disease: initial experience with 18F-fluoride PET/CT and comparison between 18F-fluoride PET and 18F-fluoride PET/CT. J Nucl Med 45:272-278, 2004
114. Leventis AK, Shariat SF, Slawin KM: Local recurrence after radical prostatectomy: correlation of US features with prostatic fossa biopsy findings. Radiology 219:432-439, 2001
115. Fowler JE Jr, Brooks J, Pandey P, et al: Variable histology of anastomotic biopsies with detectable prostate specific antigen after radical prostatectomy. J Urol 153:1011-1014, 1995
116. Connolly JA, Shinohara K, Presti JC Jr, et al: Local recurrence after radical prostatectomy: characteristics in size, location, and relationship to prostate-specific antigen and surgical margins. Urology 47: 225-231, 1996
117. Albertsen PC, Hanley JA, Harlan LC, et al: The positive yield of imaging studies in the evaluation of men with newly diagnosed prostate cancer: a population based analysis. J Urol 163:1138-1143, 2000
118. Johnstone P, GJ T, Riffenburgh RH: Yield of imaging and scintigraphy assessing biochemical failure in prostate cancer patients. Urol Oncol 3:108-112, 1997
119. Kramer S, Gorich J, Gottfried HW, et al: Sensitivity of computed tomography in detecting local recurrence of prostatic carcinoma following radical prostatectomy. Br J Radiol 70:995-999, 1997
120. Cox JD, Gallagher MJ, Hammond EH, et al: Consensus statements on radiation therapy of prostate cancer: guidelines for prostate re-biopsy after radiation and for radiation therapy with rising prostate-specific antigen levels after radical prostatectomy. American Society for Therapeutic Radiology and Oncology Consensus Panel. J Clin Oncol 17: 1155, 1999
121. Turner JW, Hawes DR, Williams RD: Magnetic resonance imaging for detection of prostate cancer metastatic to bone. J Urol 149:1482-1484, 1993
122. Freedman GM, Negendank WG, Hudes GR, et al: Preliminary results of a bone marrow magnetic resonance imaging protocol for patients with high-risk prostate cancer. Urology 54:118-123, 1999
123. Sella T, Schwartz LH, Swindle PW, et al: Suspected local recurrence after radical prostatectomy: endorectal coil MR imaging. Radiology 231:379-385, 2004
124. Silverman JM, Krebs TL: MR imaging evaluation with a transrectal surface coil of local recurrence of prostatic cancer in men who have undergone radical prostatectomy. Am J Roentgenol 168:379-385, 1997
125. Ornstein DK, Colberg JW, Virgo KS, et al: Evaluation and management of men whose radical prostatectomies failed: results of an international survey. Urology 52:1047-1054, 1998
126. Cher ML, Bianco FJ Jr., Lam JS, et al: Limited role of radionuclide bone scintigraphy in patients with prostate specific antigen elevations after radical prostatectomy. J Urol 160:1387-1391, 1998
127. Kane CJ, Amling CL, Johnstone PA, et al: Limited value of bone scintigraphy and computed tomography in assessing biochemical failure after radical prostatectomy. Urology 61:607-611, 2003
128. Sabbatini P, Larson SM, Kremer A, et al: Prognostic significance of extent of disease in bone in patients with androgen-independent prostate cancer. J Clin Oncol 17:948-957, 1999
129. Noguchi M, Kikuchi H, Ishibashi M, et al: Percentage of the positive area of bone metastasis is an independent predictor of disease death in advanced prostate cancer. Br J Cancer 88:195-201, 2003
130. Rigaud J, Tiguert R, Le Normand L, et al: Prognostic value of bone scan in patients with metastatic prostate cancer treated initially with androgen deprivation therapy. J Urol 168:1423-1426, 2002
131. Antoch G, Vogt FM, Freudenberg LS, et al: Whole-body dual-modality PET/CT and whole-body MRI for tumor staging in oncology. JAMA 290:3199-3206, 2003
132. Panel ASfTRaOC: Consensus Statements on Radiation Therapy of Prostate Cancer: Guidelines for Prostate Re-Biopsy After Radiation and for Radiation Therapy With Rising Prostate-Specific Antigen Levels After Radical Prostatectomy. J Clin Oncol 17:1155-1163, 1999
133. Petrylak DP: Chemotherapy for advanced hormone refractory prostate cancer. Urology 54:30-35, 1999
134. Khan MA, Carducci MA, Partin AW: The evolving role of docetaxel in the management of androgen independent prostate cancer. J Urol 170:1709-1716, 2003
135. Eisenberger MA, Blumenstein BA, Crawford ED, et al: Bilateral orchiectomy with or without flutamide for metastatic prostate cancer. N Engl J Med 339:1036-1042, 1998
136. Seckin B, Anthony CT, Murphy B, et al: Can prostate-specific antigen be used as a valid end point to determine the efficacy of chemotherapy for advanced prostate cancer? World J Urol 14:S26-S29, 1996 (suppl 1)
137. Schneider JA, Divgi CR, Scott AM, et al: Flare on bone scintigraphy following Taxol chemotherapy for metastatic breast cancer. J Nucl Med 35:1748-1752, 1994
138. McNeil BJ: Value of bone scanning in neoplastic disease. Semin Nucl Med 14:277-286, 1984
139. Oyama N, Akino H, Suzuki Y, et al: FDG PET for evaluating the change of glucose metabolism in prostate cancer after androgen ablation. Nucl Med Commun 22:963-969, 2001
140. Oyama N, Kim J, Jones LA, et al: MicroPET assessment of androgenic control of glucose and acetate uptake in the rat prostate and a prostate cancer tumor model. Nucl Med Biol 29:783-790, 2002
141. Oyama N, Ponde DE, Dence C, et al: Monitoring of therapy in androgen-dependent prostate tumor model by measuring tumor proliferation. J Nucl Med 45:519-525, 2004
142. Shimizu N, Masuda H, Yamanaka H, et al: Fluorodeoxyglucose positron emission tomography scan of prostate cancer bone metastases with flare reaction after endocrine therapy. J Urol 161:608-609, 1999
143. Wong RJ, Lin DT, Schoder H, et al: Diagnostic and prognostic value of [(18)F]fluorodeoxyglucose positron emission tomography for recurrent head and neck squamous cell carcinoma. J Clin Oncol 20:4199-4208, 2002
144. Vansteenkiste JF, Stroobants SG, Dupont PJ, et al: Prognostic importance of the standardized uptake value on (18)F-fluoro-2-deoxy-glucose-positron emission tomography scan in non-small-cell lung cancer: An analysis of 125 cases. Leuven Lung Cancer Group. J Clin Oncol 17:3201-3206, 1999
145. Eary JF, O'Sullivan F, Powitan Y, et al: Sarcoma tumor FDG uptake measured by PET and patient outcome: a retrospective analysis. Eur J Nucl Med Mol Imaging 29:1149-1154, 2002
146. Oyama N, Akino H, Suzuki Y, et al: Prognostic value of 2-deoxy-2-[F-18]fluoro-D-glucose positron emission tomography imaging for patients with prostate cancer. Mol Imaging Biol 4:99-104, 2002
147. Motzer RJ, Bander NH, Nanus DM: Renal-cell carcinoma. N Engl J Med 335:865-875, 1996

148. Hilton S: Imaging of renal cell carcinoma. Semin Oncol 27:150-159, 2000
149. Schreyer HH, Uggowitzer MM, Ruppert-Kohlmayr A: Helical CT of the urinary organs. Eur Radiol 12:575-591, 2002
150. Kopka L, Fischer U, Zoeller G, et al: Dual-phase helical CT of the kidney: Value of the corticomedullary and nephrographic phase for evaluation of renal lesions and preoperative staging of renal cell carcinoma. AJR Am J Roentgenol 169:1573-1578, 1997
151. Zagoria RJ, Bechtold RE, Dyer RB: Staging of renal adenocarcinoma: role of various imaging procedures. Am J Roentgenol 164:363-370, 1995
152. Margaritora S, Porziella V, D'Andrilli A, et al: Pulmonary metastases: can accurate radiological evaluation avoid thoracotomic approach? Eur J Cardiothorac Surg 21:1111-1114, 2002
153. Diederich S, Semik M, Lentschig MG, et al: Helical CT of pulmonary nodules in patients with extrathoracic malignancy: CT-surgical correlation. Am J Roentgenol 172:353-360, 1999
154. Wahl RL, Harney J, Hutchins G, et al: Imaging of renal cancer using positron emission tomography with 2-deoxy-2-(18F)-fluoro-D-glucose: pilot animal and human studies. J Urol 146:1470-1474, 1991
155. Bachor R, Kotzerke J, Reske SN, et al: [Lymph node staging of bladder neck carcinoma with positron emission tomography]. Urologe A 38: 46-50, 1999
156. Ramdave S, Thomas GW, Berlangieri SU, et al: Clinical role of F-18 fluorodeoxyglucose positron emission tomography for detection and management of renal cell carcinoma. J Urol 166:825-830, 2001
157. Kang DE, White RL Jr, Zuger JH, et al: Clinical use of fluorodeoxyglucose F 18 positron emission tomography for detection of renal cell carcinoma. J Urol 171:1806-1809, 2004
158. Miyakita H, Tokunaga M, Onda H, et al: Significance of 18F-fluorodeoxyglucose positron emission tomography (FDG-PET) for detection of renal cell carcinoma and immunohistochemical glucose transporter 1 (GLUT-1) expression in the cancer. Int J Urol 9:15-18, 2002
159. Leibovich BC, Blute ML, Cheville JC, et al: Prediction of progression after radical nephrectomy for patients with clear cell renal cell carcinoma: a stratification tool for prospective clinical trials. Cancer 97: 1663-1671, 2003
160. Ficarra V, Righetti R, Pilloni S, et al: Prognostic factors in patients with renal cell carcinoma: retrospective analysis of 675 cases. Eur Urol 41:190-198, 2002
161. Kavolius JP, Mastorakos DP, Pavlovich C, et al: Resection of metastatic renal cell carcinoma. J Clin Oncol 16:2261-2266, 1998
162. Raj GV, Partin AW, Polascik TJ: Clinical utility of indium 111-capromab pendetide immunoscintigraphy in the detection of early, recurrent prostate carcinoma after radical prostatectomy. Cancer 94: 987-996, 2002
163. Jadvar H, Kherbache HM, Pinski JK, et al: Diagnostic role of [F-18]-FDG positron emission tomography in restaging renal cell carcinoma. Clin Nephrol 60:395-400, 2003
164. Safaei A, Figlin R, Hoh CK, et al: The usefulness of F-18 deoxyglucose whole-body positron emission tomography (PET) for re-staging of renal cell cancer. Clin Nephrol 57:56-62, 2002
165. Majhail NS, Urbain JL, Albani JM, et al: F-18 fluorodeoxyglucose positron emission tomography in the evaluation of distant metastases from renal cell carcinoma. J Clin Oncol 21:3995-4000, 2003
166. Dalbagni G, Genega E, Hashibe M, et al: Cystectomy for bladder cancer: a contemporary series. J Urol 165:1111-1116, 2001
167. Ghoneim MA, el-Mekresh MM, el-Baz MA, et al: Radical cystectomy for carcinoma of the bladder: Critical evaluation of the results in 1,026 cases. J Urol 158:393-399, 1997
168. Stein JP, Lieskovsky G, Cote R, et al: Radical cystectomy in the treatment of invasive bladder cancer: long-term results in 1,054 patients. J Clin Oncol 19:666-675, 2001
169. Frank I, Cheville JC, Blute ML, et al: Transitional cell carcinoma of the urinary bladder with regional lymph node involvement treated by cystectomy: Clinicopathologic features associated with outcome. Cancer 97:2425-2431, 2003
170. Paik ML, Scolieri MJ, Brown SL, et al: Limitations of computerized tomography in staging invasive bladder cancer before radical cystectomy. J Urol 163:1693-1696, 2000
171. Yaman O, Baltaci S, Arikan N, et al: Staging with computed tomography, transrectal ultrasonography and transurethral resection of bladder tumour: Comparison with final pathological stage in invasive bladder carcinoma. Br J Urol 78:197-200, 1996
172. Jager GJ, Barentsz JO, Oosterhof GO, et al: Pelvic adenopathy in prostatic and urinary bladder carcinoma: MR imaging with a three-dimensional TI-weighted magnetization-prepared-rapid gradient-echo sequence. AJR Am J Roentgenol 167:1503-1507, 1996
173. Kim B, Semelka RC, Ascher SM, et al: Bladder tumor staging: comparison of contrast-enhanced CT, T1- and T2-weighted MR imaging, dynamic gadolinium-enhanced imaging, and late gadolinium-enhanced imaging. Radiology 193:239-245, 1994
174. de Jong IJ, Pruim J, Elsinga PH, et al: Visualisation of bladder cancer using (11)C-choline PET: first clinical experience. Eur J Nucl Med Mol Imaging 29:1283-1288, 2002
175. Kosuda S, Kison PV, Greenough R, et al: Preliminary assessment of fluorine-18 fluorodeoxyglucose positron emission tomography in patients with bladder cancer. Eur J Nucl Med 24:615-620, 1997
176. Schoder H, Erdi YE, Larson SM, et al: PET/CT: A new imaging technology in nuclear medicine. Eur J Nucl Med Mol Imaging 30:1419-1437, 2003
177. Bar-Shalom R, Yefremov N, Guralnik L, et al: Clinical performance of PET/CT in evaluation of cancer: additional value for diagnostic imaging and patient management. J Nucl Med 44:1200-1209, 2003
178. Ahlstrom H, Malmstrom PU, Letocha H, et al: Positron emission tomography in the diagnosis and staging of urinary bladder cancer. Acta Radiol 37:180-185, 1996
179. Deloar HM, Fujiwara T, Nakamura T, et al: Estimation of internal absorbed dose of L-[methyl-11C]methionine using whole-body positron emission tomography. Eur J Nucl Med 25:629-633, 1998
180. Seltzer MA, Jahan SA, Sparks R, et al: Radiation dose estimates in humans for (11)C-acetate whole-body PET. J Nucl Med 45:1233-1236, 2004

Lung Cancer xxx (2009) xxx–xxx

Contents lists available at ScienceDirect

Lung Cancer

journal homepage: www.elsevier.com/locate/lungcan

Limitations of dual time point PET in the assessment of lung nodules with low FDG avidity

Francis J. Cloran[a,b], Kevin P. Banks[a,*], Won S. Song[a], Young Kim[a,b], Yong C. Bradley[a]

[a] Brooke Army Medical Center, Department of Radiology, 3851 Roger Brooke Drive, Fort Sam Houston, TX 78234, United States
[b] Wilford Hall Medical Center, Department of Radiology, 2200 Bergquist Drive, Lackland Air Force Base, TX 78236, United States

ARTICLE INFO

Article history:
Received 26 February 2009
Received in revised form 5 May 2009
Accepted 20 May 2009

Keywords:
Dual time point
Delayed imaging
Positron emission tomography
Lung cancer
Lung nodule
SUV

ABSTRACT

FDG PET has long shown efficacy in the evaluation of indeterminate pulmonary nodules. More recently, the use of dual time point imaging has been looked at as a means for improving sensitivity and accuracy. While initial reports were very promising, more recent results looking specifically at pulmonary lesions with low levels of FDG avidity demonstrated limitations. These lesions (initial maximum standard uptake value of less than 2.5) are of particular interest due to the fact that well-differentiated adenocarcinomas, broncheoaveolar carcinoma and carcinoid may have low FDG avidity on standard PET imaging, leading to false-negative exams. Our study retrospectively reviewed the accuracy of dual time point (DTP) FDG PET imaging to determine if it aided in the identification of malignant pulmonary nodules when initial time point imaging showed a maximum SUV of less than 2.5. 113 patients had undergone a total of 130 DTP PET/CT with 152 lesions assessed. 67 lesions were subsequently definitively diagnosed as benign or malignant based upon biopsy or imaging follow-up. Utilizing a maximum SUV increase of 10%, which optimizes our sensitivity and specificity; our results demonstrate a sensitivity of 63% and a specificity of 59%, similar to other investigators evaluating lesions with low FDG avidity. Increasing or decreasing this threshold did not improve our results, nor did the addition of lesions with maximum SUV's of 2.5 or greater on initial imaging. Specifically in nodules with low FDG avidity (max SUV < 2.5), the sensitivity was 61%, specificity 58%, and accuracy was 60%. Our findings suggest that DTP FDG PET may not be of benefit in the assessment of pulmonary nodules with maximum SUV of less than 2.5 on initial imaging.

Published by Elsevier Ireland Ltd.

1. Introduction

18F-FDG PET has repeatedly demonstrated its utility for differentiating benign and malignant lung lesions. Typically, malignant pulmonary nodules will have increased FDG uptake due to overexpression of glucose transporter I [1]. In addition, the intracellular concentration of hexokinase is elevated which assists in the trapping of FDG within these malignant cells. Unfortunately, inflammatory processes have the same mechanism of action and cannot be easily distinguished from malignancy [2]. In theory, benign pulmonary nodules should not overexpress either glucose transporter I or hexokinase and thereby should not have increased FDG avidity. Unfortunately, some well-differentiated malignancies (classically, bronchoalveolar carcinoma, well-differentiated adenocarinoma, and carcinoid tumors) may not demonstrate increased FDG avidity [3]. Further confounding the issue is that some benign inflammatory and infectious processes can demonstrate increased FDG avidity as well [2]. In order to distinguish whether a low FDG avid pulmonary nodule (maximum SUV (max SUV) < 2.5 on initial imaging) is benign or malignant, dual time point imaging has been used [4,5]. Theoretically, over a short time frame, malignant nodules would continue to accumulate and trap FDG as opposed to benign processes which would either maintain stable or even decreased FDG activity [2].

Some authors found dual-time-point imaging may improve the sensitivity and/or specificity of FDG PET and thus have the potential to improve accuracy in the evaluation of lung nodules [2,6,7]. Others recently have shown less promising results when looking specifically at lesions with low FDG avidity [8]. The purpose of our study was to further investigate the accuracy of dual time point FDG PET imaging for determining the nature of pulmonary lesions when the initial 1 h maximum SUV is less than 2.5.

2. Materials and methods

All reports from PET/CT examination using dual time point (DTP) technique performed at our institution from the period of June 2006 to September 2008 were retrospectively reviewed.

* Corresponding author. Tel.: +1 210 916 1906; fax: +1 210 916 1967.
E-mail address: kevin.banks@amedd.army.mil (K.P. Banks).

0169-5002/$ – see front matter. Published by Elsevier Ireland Ltd.
doi:10.1016/j.lungcan.2009.05.013

Institutional review board (IRB) approval was obtained for this research and patient consent was waived due to the retrospective nature of the study.

The goal of the activity was to quantify the diagnostic benefit of DTP. During this 15-month period, 113 patients underwent a total of 130 DTP PET/CT with 152 lesions assessed. Patients were referred for PET/CT as part of their routine clinical management for either initial assessment of an indeterminate pulmonary nodule(s) without history of known malignancy, initial assessment of an indeterminate pulmonary nodule(s) with history of known non-pulmonary malignancy, follow-up of indeterminate pulmonary nodule(s), or concern for recurrence in individuals with a personal history of lung cancer.

Imaging from vertex of the head to mid thighs was obtained using an integrated in-line PET/CT scanner (Biograph; Siemens Medical Solutions USA, Inc., Hoffman Estates, IL). PET was performed in the fasting state using F-18 FDG (PETNET Solutions, Hoffman Estates, IL) with a prescribed dose of 12–18 mCi (average 16.5 ..mCi). At approximately 60 min (average 64 min) following injection of radiopharmaceutical, whole body CT during quiet respiration was performed (skull base to mid thighs) immediately followed by PET. Data acquisition for the CT was obtained using 130 kV_p, 125–135 mA, 5-mm pitch, and 0.8 s tube rotation. Reconstructed images were obtained by ordered-subset expectation maximization (OSEM) technique using 8 subsets and 2 iterations in a 128 × 128 matrix for PET and 512 × 512 matrix for CT. Intravenous contrast (Isovue 300, 100 cc, 1.5 cc/s, Bracco Diagnostics, Princeton, NJ) was administered at the ordering provider's discretion and absence of any patient contraindications. Emission scanning for the PET was performed moving caudal to cranial with 2–4 min/bed acquisitions (weight based determination).

After time point 1 was completed, images were reviewed by the nuclear medicine physician who determined if dual time point assessment was indicated. In general at our institution, DTP imaging was not considered indicated in markedly FDG-avid lesions (>5.0 max SUV). When DTP was indicated, 2 h following injection (average 121 min post injection), a second CT was obtained (limited to the chest) followed by repeat PET of the chest. No significant difference in acquisition times was present between patients with benign versus malignant lesions.

Five nuclear medicine physicians were involved in the interpretation of the studies. All were fellowship trained and board certified in nuclear medicine with an average of 4.6 years of experience interpreting PET/CT. Maximum SUVs were determined based upon original reported values. Both regions of interest (ROI) and volume of interest (VOI) techniques were used for measurement based upon the individual interpreting providers preference. If ROI technique was utilize, the slice demonstrating maximum intensity by visual assessment was measured as well as the level above and below and greatest value reported. Of 130 examinations, 7 reports (10 lesions) were subsequently excluded from analysis because the original interpreting nuclear medicine physician did not include DTP data in the findings. Another 7 exams (14 lesions) were also excluded due to being performed to evaluate for response to chemotherapy or radiation therapy which the authors felt would induce error into DTP analysis.

Sixty-seven of the 128 lesions were able to be diagnosed as either benign or malignant nature (Table 1).

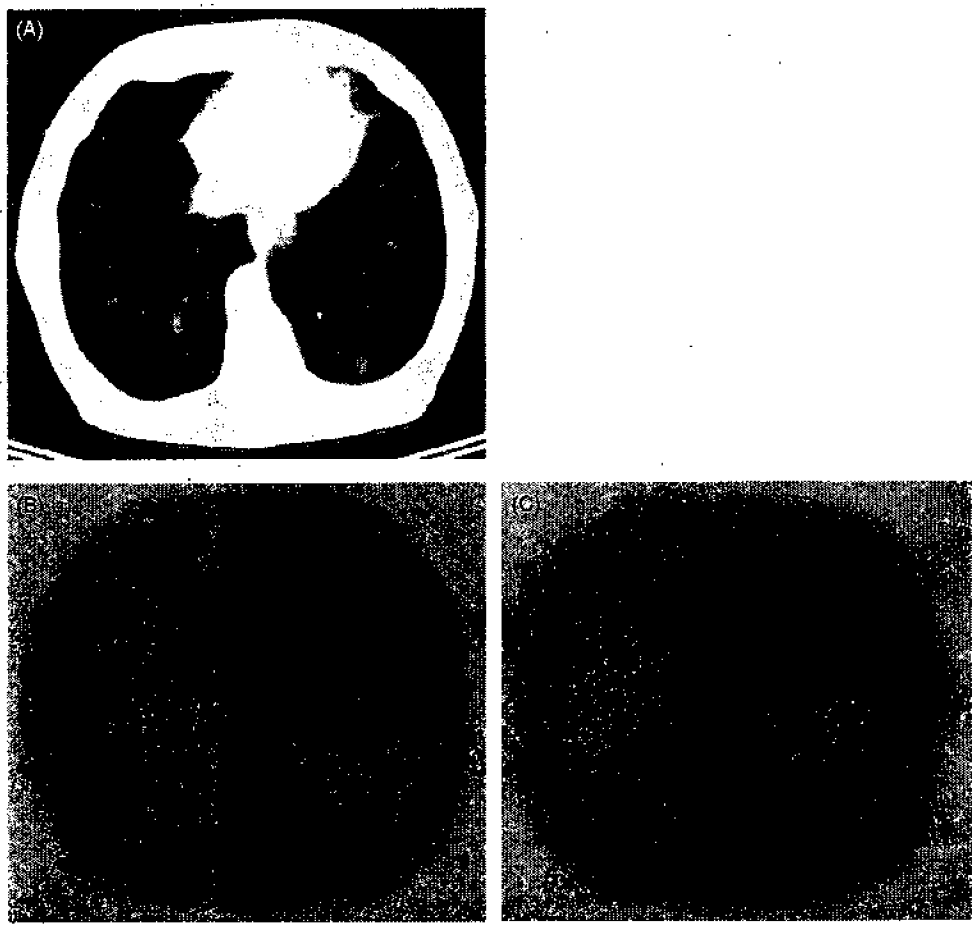

Fig. 1. True positive DTP result. Noncontrast axial CT (A) shows a 1.0 cm indeterminate left lower lobe pulmonary nodule with max SUV of 1.3 on initial imaging (B) which increased to 1.9 at second time point (C) for a +46.2% change. Biopsy showed NSCLCa NOS.

Please cite this article in press as: Cloran FJ, et al. Limitations of dual time point PET in the assessment of lung nodules with low FDG avidity. Lung Cancer (2009), doi:10.1016/j.lungcan.2009.05.013

Table 1
Type of pulmonary lesions included in DTP analysis. (NOS = not otherwise specified NTMB = nontuberculous mycobacterium).

	Malignant	Benign
Pathology		
Adenocarcinoma	13	
NSCLCa NOS	8	
Small cell	5	
Bronchoaveolar Carcinoma	4	
Squamous cell	2	
Metastasis	1	
Large cell	1	
Focal fibrosis		7
Infection		
Fungal		3
NTMB		1
Organizing pneumonia		2
Solitary fibrous tumor		2
Eosinophilic granuloma		1
Interval progression	4	
Interval improvement		10
2 year stability		3
Total	38	29

Determination of benignity or malignancy of lesions was based upon one of four criteria: (1) histology in cases of tissue sampling (50 lesions–34 malignant (Figs. 1 and 2) and 16 benign (Figs. 3 and 4), (2) progression of lesion with history of malignancy elsewhere (4 lesions), (3) improvement of lesion without intervening oncologic therapy (10 lesions), or (4) 2 years or more of stability by CT examination without intervening oncologic therapy (3 lesions). Sixty of the lesions did not meet any of these four criteria and were excluded from analysis. One lesion was excluded due to the proximity of the lateral wall of the left ventricle and subsequent inability to perform accurate quantitative analysis due to the heart's physiologic activity.

3. Results

A total of 67 lesions were assessed with subsequent definitive diagnosis based upon tissue sampling or imaging follow-up. Lesion sizes measured 0.7–11.0 cm. Of these, 42 met criteria for low FDG avidity lesions with maximum SUV < 2.5 (size 0.7–3.6 cm, mean 1.6 cm). 20 of these lesions (48%) demonstrated <10% change in their avidity. 22 of these lesions (52%) demonstrated >10% change in their avidity (Tables 2 and 3). Utilizing the threshold of 10%, the resulting sensitivity is 61%, specificity is 58% and accuracy is 60%. Applying a less stringent threshold of 5%, the resulting sensitivity is 70%, specificity is 47% and accuracy is 60%. Utilizing more strict criteria, thresholds of 15% and 20%, the resulting sensitivities are 52% (15%) and 43% (20%), specificities 63% (15%) and 63% (20%) and accuracy is 57% (15%) and 52% (20%). Utilizing the threshold of 10%, the positive predictive value was 63% and the negative predictive value was 58%.

In taking in consideration all-comers (67 lesions), 31 of these lesions (46%) demonstrated <10% change in their avidity. 36 of these

Fig. 2. False negative DTP result. Noncontrast axial CT (A) shows a 0.9 cm indeterminate right lower lobe pulmonary nodule with max SUV of 2.0 on initial imaging (B) which increased to 2.1 at second time point (C) for only a +5.0% change. Biopsy showed adenocarcinoma.

Please cite this article in press as: Cloran FJ, et al. Limitations of dual time point PET in the assessment of lung nodules with low FDG avidity. Lung Cancer (2009), doi:10.1016/j.lungcan.2009.05.013

Table 2
Final diagnoses of lesions with maximum SUV < 2.5 with either less than 10% increase or greater than 10% increase in maximum SUV on DTP imaging.

Initial max SUV	Max SUV on DTP	% Change	Diagnosis
Diagnoses of lesions with max SUV < 2.5 with less than 10% increase in maximum SUV on DTP			
1.1	0.8	−27.3	BAC
1.9	1.5	−21.1	Benign
1.5	1.2	−20.0	Adenocarcinoma
1.6	1.3	−18.8	Benign
0.7	0.6	−14.3	Adenocarcinoma
0.8	0.7	−12.5	Benign
2.0	1.8	−10.0	Benign
1.6	1.5	−6.3	Benign
2.2	2.1	−4.5	Benign
0.1	0.1	0.0	Benign
0.1	0.1	0.0	Benign
0.1	0.1	0.0	Benign
0.7	0.7	0.0	Adenocarcinoma
1.4	1.4	0.0	NSCLCa
1.6	1.6	0.0	BAC
2.0	2.1	5.0	Adenocarcinoma
1.7	1.8	5.9	Squamous cell Carcinom
1.4	1.5	7.1	Benign
1.2	1.3	8.3	Benign
Diagnoses of lesions with max SUV < 2.5 with greater than 10% increase in maximum SUV on DTP			
1.8	2.0	11.1	Adenocarcinoma
1.7	1.9	11.8	Adenocarcinoma
0.7	0.8	14.3	Benign
2.0	2.3	15.0	NSCLCa
1.1	1.3	18.2	Adenocarcinoma
1.5	1.8	20.0	NSCLCa
1.4	1.7	21.4	Adenocarcinoma
2.1	2.6	23.8	Benign
0.8	1.0	25.0	Benign
2.2	2.8	27.3	Benign
1.7	2.2	29.4	Adenocarcinoma
2.0	2.7	35.0	Adenocarcinoma
2.2	3.0	36.4	Benign
1.0	1.4	40.0	Benign
0.9	1.3	44.4	Adenocarcinoma
1.3	1.9	46.2	Benign
1.3	1.9	46.2	NSCLCa
1.5	2.2	46.7	NSCLCa
1.9	2.8	47.4	Benign
0.9	1.4	55.6	BAC
0.5	1.0	100.0	BAC
2.2	5.1	131.8	Large cell

Table 3
Final diagnoses of lesions with max SUV > 2.5 with either decreasing or increasing max SUV on DTP imaging.

Initial max SUV	Max SUV on DTP	% change	Diagnosis
Diagnoses of lesions with max SUV > 2.5 with interval decreased FDG avidity on DTP			
2.6	1.6	−38.5	Benign
2.8	2.7	−3.6	NSCLCa
3.3	2.6	−21.2	Small cell
5.8	5.3	−8.6	Adenocarcinoma
Diagnoses of lesions with max SUV > 2.5 with interval increased FDG avidity on DTP			
2.6	3.0	15.4	Benign
2.6	3.2	23.1	Lung Recur
2.6	2.9	11.5	NSCLCa
2.6	2.7	3.8	Small cell
2.7	3.0	11.1	Benign
2.9	3.1	6.9	Adenocarcinoma
2.9	3.1	6.9	Benign
2.9	3.3	13.8	Small cell
3.2	4.6	43.8	Small cell
3.8	4.4	15.8	Lung recur
4.4	4.6	4.5	Benign
5.4	5.5	1.9	Benign
5.7	6.8	19.3	NSCLCa
6.2	8.0	29.0	Met Recur
6.3	9.3	47.6	EG
7.1	8.8	23.9	Metastastic adenocarcinoma
7.1	7.6	7.0	Benign
15.2	18.8	23.7	Small cell

lesions (54%) demonstrated >10% change in their avidity. Utilizing the threshold of 10%, the resulting sensitivity is 63%, specificity is 59% and accuracy is 61% with a positive predictive value of 64% and negative predictive value of 55% (Table 4).

4. Discussion

In general, utilization of SUVs in PET has become an accepted practice and useful adjunct in the clinical management of pulmonary nodules, where metabolic activity correlated with likelihood of malignancy [4]. An accepted practice in the evaluation of pulmonary nodules is that those which demonstrate a maximum SUV of greater than 2.5 are suspicious for malignancy in the appropriate clinical setting [5]. However, there are numerous reports of malignant nodules which are non-FDG avid such as bronchoalveolar carcinoma which typically demonstrate maximum SUVs < 2.5 [3] and benign entities such as infectious or inflammatory nodules which demonstrate maximum SUVs of >2.5 [9].

In 2001, Zhuang et al, proposed utilizing dual time point FDG PET imaging to differentiate thoracic malignant from benign processes with promising initial results based on changes in the average SUV [2]. Matthies et al published supportive data in 2002 demonstrating that dual-point imaging for all-comers (SUV independent) with pulmonary lesions was 100% sensitive and 89% specific for detection of thoracic malignancy when a 10% threshold was adopted (i.e., a 10% or greater rise in SUV from initial SUV to the second SUV) [6]. In 2007, Xiu et al demonstrated in a study of 46 patients with non-FDG avid nodules (SUV < 2.5) that utilizing a 10% threshold for dual point imaging yielded a sensitivity of 81% and a specificity of 87% for detection of malignant nodule. His results raised

Table 4
Distribution of DTP results for malignant and benign lesions. All lesions (top) and results limited to low FDG avidity lesions with max SUV <2.5 on TP1 (time point 1 (initial imaging performed after approximately 60 min after injection of FDG)) (bottom).

	All lesions		
	# Lesions	Average TP1 (mSUV)	Average % increase
>10% increase on DTP			
Malignant	24	3.0	34.4
Benign	12	2.2	30.5
<10% increase on DTP			
Malignant	14	2.2	−4.9
Benign	17	2.2	−4.5

Sensitivity 63%, specificity 59%, accuracy 61%
NPV 55%, PPV 64%

Lesions with TP1 <2.5 max SUV

	# Lesions	Average TP1 (mSUV)	Average % increase
>10% increase on DTP			
Malignant	14	1.5	41.9
Benign	8	1.5	32.5
<10% increase on DTP			
Malignant	9	1.5	−5.2
Benign	11	1.2	

Sensitivity 61%, specificity 58%, accuracy 60%
NPV 55%, PPV 64%

Please cite this article in press as: Cloran FJ, et al. Limitations of dual time point PET in the assessment of lung nodules with low FDG avidity. Lung Cancer (2009), doi:10.1016/j.lungcan.2009.05.013

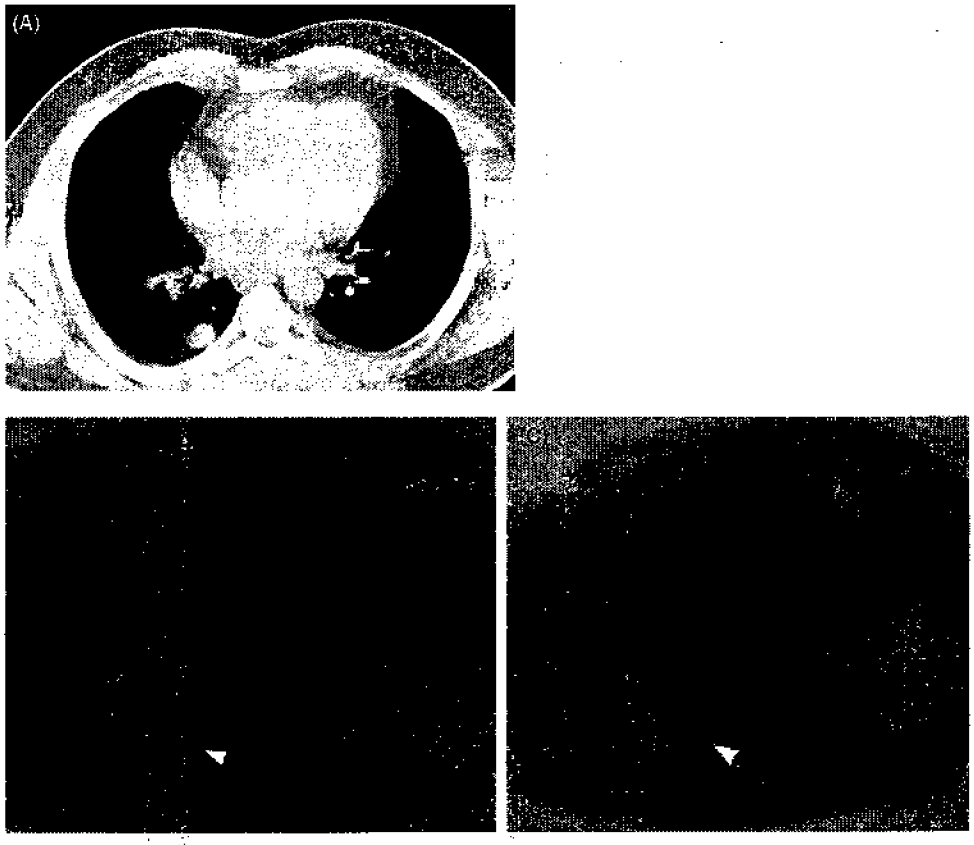

Fig. 3. True negative DTP result. Noncontrast axial CT (A) shows a 1.9 cm indeterminate right lower lobe pulmonary nodule with max SUV of 1.9 on initial imaging (B) which decreased to 1.5 at second time point (C) for a −21.1% change. Biopsy showed organizing pneumonia.

hope that dual point imaging could provide an accurate means for identifying malignant pulmonary nodules with low FDG avidity. Unfortunately, in contradistinction, Chen et al published a study of 31 non-avid FDG pulmonary lesions which demonstrated a specificity of 62% and a sensitivity of 40% utilizing a 10% threshold [8].

Analysis of our results demonstrates similar findings to Chen et al; that the use of dual-time point imaging does not provide a significant improvement in distinguishing malignant versus benign nodules with low FDG avidity. Specifically, in nodules with a maximum SUV of less than 2.5, the change in max SUV did not lead to the correct end-diagnosis. Utilizing a 10% threshold which optimizes our sensitivity and specificity, our results demonstrate a sensitivity of 61% and a specificity of 58% which is consistent with Chen et al (Table 4) [8]. Adjusting the threshold to 5%, 15% and 20% did not demonstrate significant changes in the specificity, sensitivity or accuracy and does not improve the utilization of dual point imaging as a tool in clarifying the malignant/benign characteristics of a pulmonary lesion. Additionally, our study population, in contradistinction to Chen et al, demonstrated a preponderance of non-granulomatous infections in our benign nodules, which may broaden the applicability of Chen's reported findings to populations where granulomatous infections are not endemic. Our results therefore do not support the use of dual time point imaging for further assessment of non FDG-avid nodules.

As has been reported by Chen and colleagues, DTP imaging for pulmonary nodules with maximum SUV of less than 2.5 is not helpful in determining a final diagnosis [8]. Although prior studies have suggested the utility of DTP imaging in pulmonary nodules [2,6,7] our results did not demonstrate the same conclusions. Selection criteria may in part be responsible for the differences in our results. Prior studies have included patients with nodules with initial maximum SUV greater than 2.5 [6]. We feel that it is possible that the physiologic differences between FDG avid and non FDG-avid nodules (upregulation of glucose transporter 1 and increased hexoskinase expression), may be the same factors which impact changes in FDG uptake over the course of multiple time point determinations. Thus, lesions which have increased GLUT1 and hexoskinase will tend to be more FDG avid on standard PET imaging and, likewise, tend to demonstrate increasing activity on dual time point imaging. Additionally, some of the prior studies on this topic had a patient population with low prevalence of granulomatous disease [7] or only investigated patients with known malignancies [2].

Our study did have limitations. For example, the data was based on retrospective data and did not reflect ideal prospective data; however, we do not believe that a prospective design would have significantly altered our findings. Additionally, the total number of lesions which qualified as non FDG-avid was somewhat low (45); however, larger than Chen et al (31). A larger population sampling may demonstrate subgroups of non FDG-avid nodules which may demonstrate radiographic characteristics which may make the utilization of dual time point imaging useful. Third, our study utilized FDG as the marker for increased avidity; employing other radiopharmaceuticals in conjunction with FDG may demonstrate utility in differentiating benign from malignant etiologies in non FDG avid pulmonary lesions.

In conclusion, our preliminary data is consistent with the recently released results of Chen and supports the idea that dual time point PET is unsatisfactory for assessing whether or not a non FDG-avid pulmonary nodule is malignant.

Please cite this article in press as: Cloran FJ, et al. Limitations of dual time point PET in the assessment of lung nodules with low FDG avidity. Lung Cancer (2009), doi:10.1016/j.lungcan.2009.05.013

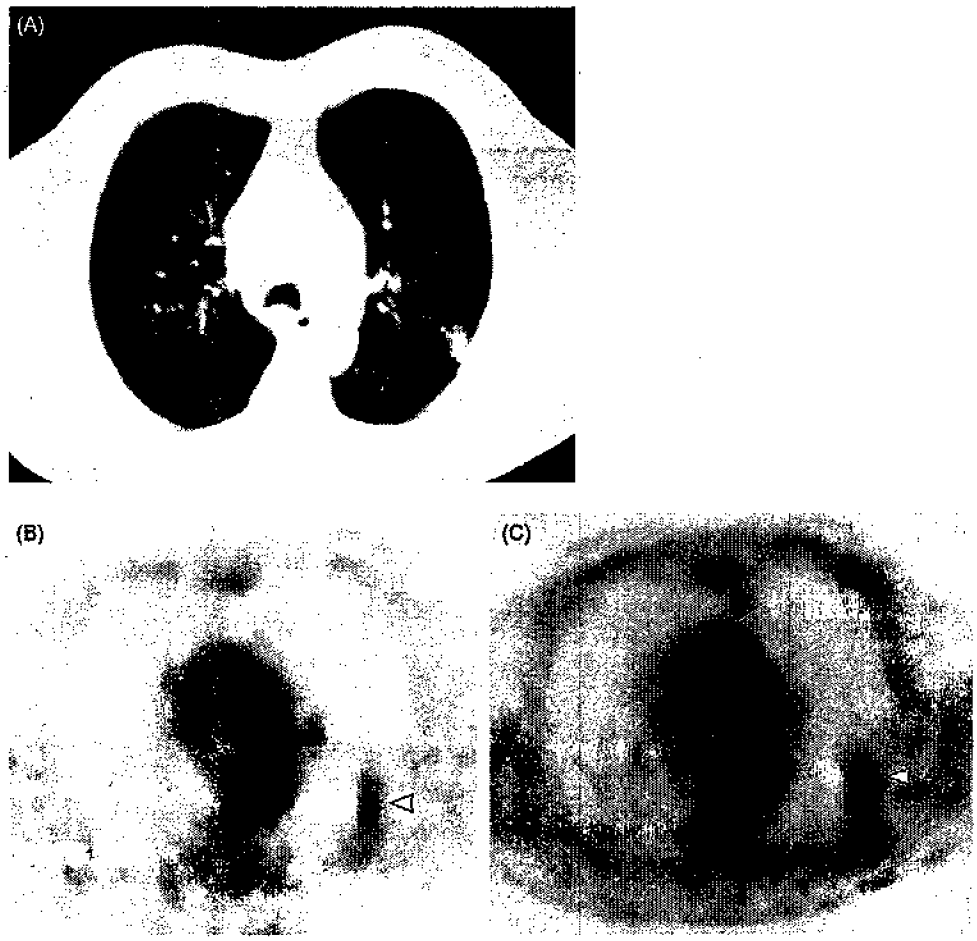

Fig. 4. False positive DTP result. Noncontrast axial CT (A) shows a 1.2 cm indeterminate left upper lobe pulmonary nodule with max SUV of 1.9 on initial imaging (B) which increased to 2.8 at second time point (C) for a +47.4% change. Biopsy showed focal fibrosis.

5. Conflict of interest statement

None of the authors have any actual or potential conflicts of interest to declare.

References

[1] Mochizuki T, Tsukamoto E, Kuge Y, et al. FDG uptake and glucose transporter subtype expressions in experimental tumor and inflammation models. J Nucl Med 2001;42:1551–5.
[2] Zhuang H, Pourdehnad M, Lambright E, et al. Dual time point 18F-FDG PET imaging for differentiating malignant from inflammatory processes. J Nucl Med 2001;42:1412–7.
[3] Kotaro H, Yoshimichi U, Hiroyasu S, et al. Fluorine-18-FDG PET imaging is negative in bronchioalveolar carcinoma. J Nucl Med 1998;39:1016–20.
[4] Gould M, Maclean C, Kuschner W, et al. Accuracy of positron emission tomography for diagnosis of pulmonary nodules and mass lesions: A meta-analysis. JAMA 2001;285:914–24.
[5] Lowe V, Fletcher J, Gobar L, et al. Prospective investigation of positron emission tomography in lung nodules. J Clin Oncol 1998;16:1075–84.
[6] Matthies A, Hickeson M, Cuchiara A, et al. Dual time point 18F-FDG PET for the evaluation of pulmonary nodules. J Nucl Med 2002;43:871–5.
[7] Xiu Y, Bhutani C, Dhurairaj T, et al. Dual-time point FDG PET imaging in the evaluation of pulmonary nodules with minimally increased metabolic activity. Clin Nucl Med 2007;32:101–5.
[8] Chen C, Lee B, Yao W, et al. Dual-phase 18F-FDG PET in the diagnosis of pulmonary nodules with an initial standard uptake value less than 2.5. AJR 2008;191:475–9.
[9] Kapucu L, Meltzer C, Townsend D, Keenan R, et al. Fluorine-18-fluorodeoxyglucose uptake in pneumonia. J Nucl Med 1998;39:1267–9.

Please cite this article in press as: Cloran FJ, et al. Limitations of dual time point PET in the assessment of lung nodules with low FDG avidity. Lung Cancer (2009), doi:10.1016/j.lungcan.2009.05.013

Neuroimaging in Patients with Gliomas

Roland T. Ullrich, M.D.,[1] Lutz W. Kracht, M.D.,[1] and Andreas H. Jacobs, M.D.[1]

ABSTRACT

Improvements of radionuclide and magnetic resonance-based imaging modalities over the past decade have enabled clinicians to noninvasively assess the dynamics of disease-specific processes at the molecular level in humans. This article will provide an overview of the recent advances in multimodal molecular neuroimaging in patients with primary brain tumors. To date, a range of complementary imaging parameters have been established in the diagnosis of brain tumors. Magnetic resonance imaging (MRI) provides mostly morphological and functional information such as tumor localization, vascular permeability, cell density, and tumor perfusion. The use of positron emission tomography (PET) enables the assessment of molecular processes, such as glucose consumption, expression of nucleoside and amino acid transporters, as well as alterations of DNA and protein synthesis. Taken together, MRI and PET give complementary information about tumor biology and activity, providing an improved understanding about the kinetics of tumor growth.

KEYWORDS: Molecular imaging, glioma, PET, MRI

GRADING AND MOLECULAR ASPECTS OF PRIMARY BRAIN TUMORS

The incidence of gliomas has increased over the past 30 years, most likely due to improvements in diagnostic modalities such as neuroimaging. The most common primary brain tumors in adults are gliomas and meningiomas. The incidence of gliomas is ~6 to 8 per 100,000 with ~75% belonging to malignant subtypes. Low-grade gliomas are more frequent in younger patients, while higher-grade tumors tend to occur in older patients. According to the World Health Organization (WHO) classification, gliomas are histologically classified into astrocytic, oligodendroglial, oligoastrocytic, ependymal, choroid plexus tumors, pineal, and mixed neuronal-glial tumors.[1] The malignancy of the tumor is determined by the histological grading as recommended by the WHO. Low-grade gliomas (WHO II) are defined as diffusely infiltrative astrocytic tumors with cytological atypia; tumors containing anaplastic cell types and high mitotic activity are classified as WHO III; gliomas with additional microvascular proliferation and/or necrosis as WHO grade IV.[1] The histological grading is highly relevant to predict the patient's prognosis. The median survival of patients with WHO grade II gliomas is usually more than 5 years, whereas patients with high-grade gliomas, such as WHO grades III and IV, have median survival rates of ~2 to 3 years and less than 1 year, respectively.[1]

Up to now, treatment outcome has hardly been predictable, because of individually different molecular tumor phenotypes that are responsible for tumor growth. Glioma-specific molecular changes result in deregulation of the cell cycle, alterations of apoptosis and cell differentiation, in neovascularization as well as tumor cell migration, and invasion into the brain parenchyma. Therefore, an improved understanding of the biology of

[1]Laboratory for Gene Therapy and Molecular Imaging, Max Planck Institute for Neurological Research with Klaus-Joachim-Zülch-Laboratories, Center for Molecular Medicine (CMMC), University of Cologne and Department of Neurology at Klinikum Fulda, Germany.

Address for correspondence and reprint requests: Professor Dr. Andreas H. Jacobs, M.D., Laboratory for Gene Therapy and Molecular Imaging, MPI for Neurological Research, Gleuelerstr. 50, 50931 Cologne, Germany (e-mail: Andreas.Jacobs@nf.mpg.de).

Neuroimaging Essentials for the Clinician; Guest Editor, Rohit Bakshi, M.D.

Semin Neurol 2008;28:484–494.
DOI 10.1055/s-0028-1083696. ISSN 0271-8235.

glial tumorgenesis is highly important for the development of molecular therapeutic targets to overcome current therapeutic limitations.

In the past decade, different genetic alterations have been identified as major factors for the development of primary or secondary gliomas. The TP53 pathway plays a crucial role in tumorigenesis of low-grade astrocytoma.[2] The TP53 gene serves as a tumor suppressor gene involved in cellular processes, including cell cycle, response to DNA damage, apoptosis, and neovascularization.[3] Mutation in the TP53 gene occurs in ~50% of low-grade gliomas, resulting in a loss of its tumor suppressor function.[4] Activity of TP53 is regulated by MDM2[5] and $p14^{ARF}$ [6] and thereby, MDM2 and $p14^{ARF}$ are promising molecular treatment targets. Also, alterations in the EGFR/PTEN/AKT/mTor and the $p16^{INK4a}$/RB1 pathways, as well as loss of heterozygosity (LOH) 10q, have been shown to induce glioma progression.[7] Most importantly, molecular alterations have been identified as prognostically relevant markers of treatment response: anaplastic oligodendroglioma with LOH 1p and/or 19q are characteristically sensitive to PCV chemotherapy,[8] and as has been reported recently, coexpression of EGFRvIII and PTEN are strongly related to response to endothelial growth factor receptor (EGFR) kinase inhibitors in patients with glioblastoma.[9]

PRIMARY DIAGNOSIS IN PATIENTS WITH GLIOMAS

A summary of magnetic resonance imaging (MRI) and positron emission tomography (PET) findings in human brain tumors is given in Table 1.

Magnetic Resonance Imaging

Magnetic resonance imaging is most commonly used for the primary diagnosis of patients with brain tumors. T1- and T2-weighted MRI provide information on the localization and the extent of brain tumors, as well as on secondary tumor effects such as edema, hemorrhage, and necrosis at high spatial resolution.

Low-grade gliomas are typically hypointense on T1-weighted and hyperintense on T2-weighted and fluid-attenuated inversion-recovery (FLAIR) images. In addition, higher-grade gliomas may cause a disruption of the blood-brain barrier (BBB) resulting in gadolinium enhancement (Fig. 1). Contrast enhancement is histologically associated with high proliferating tumor tissue and neovascularization, inducing high vascular permeability. However, leakage of the BBB might also be due to toxic effects of therapeutic interventions, such as chemotherapy, radiation, and local therapeutics that cannot be differentiated from malignant progression by MRI. In this context, Scott et al recently reported that 9% of malignant gliomas did not show contrast enhancement, whereas 48% of low-grade gliomas enhanced, indicating that contrast enhancement may not allow for the exact differentiation between low- and high-grade malignant gliomas (Fig. 2).[10]

In addition to T1- and T2-weighted images, diffusion- and perfusion-weighted-imaging (DWI, PWI), dynamic contrast-enhanced (DCE) MRI, and FLAIR sequences give complementary information about the tumor biology. DWI may provide surrogate information on the cellular density of gliomas. In areas with high cell density, diffusion of water molecules is reduced because of the limited intercellular space. Therefore, highly proliferating tumor regions with high cell densities may display a decrease of the apparent diffusion coefficient (ADC).[11] Although this might suggest that ADC can be used to distinguish between tumor and peritumoral lesions, Pauleit and colleagues reported a strong overlap between ADC values in tumor and peritumoral tissue.[12] Therefore, further studies are required to investigate the correlations between biological tumor characteristics—as determined by histology—and ADC values.

Several studies suggested that the relative cerebral blood volume (rCBV) obtained by PWI provides information that is not available by conventional MR studies on tumor angiogenesis and tumor grading in patients with gliomas.[13,14] rCBV correlates with vascular EGFR expression and the histopathological grade in nonenhancing gliomas.[15] This indicates that rCBV might be helpful for glioma preoperative tumor grading as well as provide a marker for tumor angiogenesis. rCBV enables us to differentiate between brain tumors with high blood supply from tumors with low blood supply, as well as abscesses from high-grade gliomas and metastases.[16]

Dynamic contrast-enhanced imaging acquires a series of MR images before, during, and after contrast agent injection. The serial acquisition of MR images allows the calculation of kinetic constants determining the distribution of the agent within the tumor, providing information about the exchange between the compartments' "tumor" and "blood vessels." K^{trans} serves as a marker for the assessment of leakage of the BBB, and is thereby related to angiogenesis. The vascular hyperpermeability of tumor vessels for macromolecular solutes yields a proteinaceous exudate within the tumor interstitium that is considered a favorable milieu for the in-growth of new capillary buds. Changes in tumor vessel permeability as determined by DCE MRI enable us to monitor angiogenesis and allow the prediction of pathologic tumor grade at high sensitivity.[17–19]

Magnetic Resonance Spectroscopy

Complementary to the above-described MR techniques, MR spectroscopy (MRS) reveals additional information

on cell membrane metabolism, neuronal integrity, and energy metabolism. Metabolic changes on MRS enable the differentiation between low- and high-grade glioma.[19] Metabolic products, such as N-acetylaspartate (NAA), creatine, choline, and lactate, are commonly used for the characterization of brain tumors. Increased choline values are associated with histological glioma grade and expression of the proliferation marker K_i-67.[20]

Table 1 Types of Brain Tumors and Their Characteristics in MRI/CT, [^{18}F]FDG, and [^{11}C]MET PET

Tumor Type	Signal in MRI/CT	FDG (CMRGlc)	MET Uptake Ratio
Glioma			
Pilocytic astrocytoma WHO I° (<3%)	Cystic tumor with focal contrast enhancement	Variable, focally increased	Up to 2-fold
Astrocytoma WHO II° (<5%)	T1: Slightly hypointense T2: Hyperintense	Decreased	1- to 2-fold
Anaplastic astrocytoma WHO III° (<5%)	T1: Hypointense T2: Hyperintense Contrast enhancement and perifocal edema	Variable	2- to 3-fold
Glioblastomas WHO IV° (20–25%)	Irregular tumor border T1: Central necrosis hypointense T2: Perifocal edema hyperintense contrast enhancement	Increased	>2.5-fold
Oligodendroglioma WHO II°/III° (<5%)	Inhomogeneous tumor with focal contrast enhancement and calcifications on CCT in 70–90%	Decreased/Increased	>2.5-fold >2.5-fold
Oligodendroglioma WHO II°/III°	Inhomogeneous tumor with focal contrast enhancement and calcifications on CCT in 70–90%	Decreased/Increased	>2.5-fold
Oligoastrocytoma WHO II°/III° (<5%)		Decreased/Increased	2- to 3-fold
Ependymomas (2–3%)	Characteristic localization in fourth ventricle or intramedullary; heterogenous, cystic, hemorrhages	Decreased	1.3- to 2.7-fold
Plexus papilloma (<1%)	Characteristic localization in ventricles; sharp tumor border; gross contrast enhancement	n.a.	n.a.
Gliomatosis cerebri	Diffusely infiltrating; hyperintense (T2, FLAIR)	n.a.	n.a.
Neuronal and Glioneuronal Tumors			
Dysembryoplastic neuroepithelial tumor (<1%)	Multicystic subcortical tumors with focal contrast enhancement	Decreased benzodiacepine receptor density as possible reason for epileptogenic focus	
Dysplastic gangliocytoma (<1%)		Increased	Increased
Ganglioglioma (<1%)	Cortical localization, solid or cystic with calcifications and little contrast enhancement	Variable, depending on WHO grade	n.a.
Central neurocytoma (<1%)	Sharp tumor border, inhomogenous with cysts, necroses, calcifications, positive contrast enhancement	Increased, depending on proliferative activity	Increased
Metastatic Tumors(~20% of all brain tumors)			
Lung, breast, melanoma, gastrointestinal, hypernephroma	T1 hyperintense, T2 hypointense, ring-like contrast enhancement	Variable; screening for metastasis with [^{18}F]FDG is *not* recommended	n.a.

MRI, magnetic resonance imaging, CT, computed tomography; MET, methyl-[^{11}C]-L-methionine; WHO, World Health Organization; CCT, cranial computed tomography; FLAIR, fluid-attenuated inversion-recovery.

Figure 1 Parameters of interest in the noninvasive diagnosis of brain tumors. Alteration of the blood-brain barrier and the extent of peritumoral edema are detected by MRI. Signs of increased cell proliferation can be observed by multitracer PET imaging using [^{18}F]FDG, [^{11}C]MET, and [^{18}F]FLT as specific tracers for glucose consumption, amino acid transport, and DNA synthesis, respectively. Secondary phenomena, such as inactivation of ipsilateral cortical cerebral glucose metabolism, may be observed ([^{18}F]FDG), and are of prognostic relevance. MRI, magnetic resonance imaging; PET, positron emission tomography; Gd, gadolinium. (Reproduced with permission from Jacobs A. PET in Gliomas. Stuttgart: Thieme; 2003:72–76.[74])

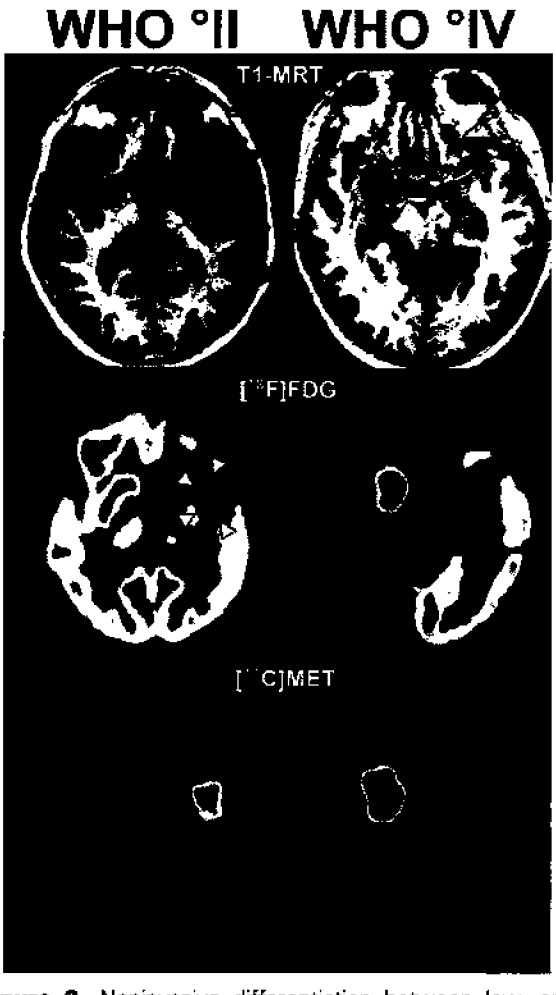

Figure 2 Noninvasive differentiation between low- and high-grade gliomas. In low-grade gliomas (WHO II), glucose metabolism is similar to white matter (arrowheads) and amino acid uptake is only moderately increased. In high-grade gliomas (GBM; WHO IV), increase of both glucose metabolism and amino acid uptake is observed. (Reproduced with permission from Jacobs A. PET in Gliomas. Stuttgart: Thieme; 2003:72–76.[74])

Creatine reflects cell energy metabolism and serves as a marker for the distinction of gliomas from metastasis, since creatine is nearly absent in metastasis.[21] High lactate concentrations might be due to non-oxidative glycolysis and are usually found in high-grade gliomas.[22] However, one major disadvantage of MRS is its low spatial resolution that cannot fully address the anatomical and biological heterogeneity of brain tumors observed by MRI.

Positron Emission Tomography

Positron emission tomography enables the in vivo measurement of metabolic and molecular processes with high sensitivity. The reader is referred to a separate article in this journal volume discussing the technical aspects of PET. In patients with brain tumors, PET provides physiological and biochemical information at the molecular level to characterize the tumor's extent, proliferative activity, metabolism, and its relation to functionally relevant parts of the brain. The most commonly used tracers in the diagnosis of brain tumors are 2-[^{18}F]fluoro-2-deoxy-D-glucose ([^{18}F]FDG), *methyl*-[^{11}C]-L-methionine ([^{11}C]MET) and 3′-deoxy-3′-[^{18}F]-fluoro-L-thymidine ([^{18}F]FLT) (Fig. 1). The accumulation of each tracer reflects the activity of its transporter via the BBB, as well as the activity of specific enzymes by which they are metabolized and trapped.

[^{18}F]FDG is phosphorylated by cellular hexokinase and is therefore a specific tracer for glucose consumption. [^{18}F]FDG is transported via the insulin-dependent glucose transporter GLUT 1 that is localized on capillary endothelial cells. The transport rate of glucose is dependent on the glucose level in the blood in accordance with the Michaelis-Menten kinetics for facilitated transport. The cellular hexokinase phosphorylates [^{18}F]FDG to [^{18}F]FDG-monophosphate that accumulates in the cell. The accumulation of

[^{18}F]FDG corresponds to high expression of GLUT1 transporter and hexokinase activity within the tumor,[23] and some cancers also show high microvessel density and high expression of the HIF1 in tumor regions with high [^{18}F]FDG uptake, indicating its role for imaging angiogenesis.[24] In brain tumors, [^{18}F]FDG-PET allows the assessment of differences in glucose metabolism among normal brain tissue, low- and high-grade gliomas, and radionecrosis.[25,26] Intratumoral glucose consumption as assessed by [^{18}F]FDG correlates with tumor grade,[27] biological aggressiveness, and prognosis of patients with primary and recurrent gliomas.[28] [^{18}F]FDG uptake in low-grade gliomas corresponds to that of normal white matter, whereas high-grade gliomas show [^{18}F]FDG uptake similar to that of the gray matter. However, [^{18}F]FDG uptake is not specific for tumor growth since [^{18}F]FDG is also metabolized in inflammatory brain lesions, focal epilepsy, and recent ischemic infarcts. Another limiting factor of [^{18}F]FDG-PET for the detection of tumor lesions is the high background activity of [^{18}F]FDG in normal cortex. Therefore, more specific tracers have been established for the diagnosis of brain tumors.

Amino acids tracers such as *methyl*-[^{11}C]-L-methionine ([^{11}C]MET), [^{11}C]-tyrosine, [^{18}F]fluoro-tyrosine, and O-(2-[^{18}F]-fluoroethyl)-L-tyrosine have been investigated as more specific radiotracers for the detection of brain tumors (Fig. 2).[29–31] The accumulation of amino acids in brain tumors is mainly due to increased transport rates mediated by type L amino acid carriers, and seems to be directly regulated by tumor growth factors.[32,33] Uptake ratios of [^{11}C]MET range between 1.2 and 6.0 in gliomas. Recent studies demonstrated that [^{11}C]MET-PET allows for the assessment of treatment effects and the differentiation of recurrent tumor from radiation necrosis.[34–36] [^{11}C]MET-PET detects parts of brain tumors as well as infiltrating areas with high sensitivity and specificity.[37] Furthermore, [^{11}C]MET uptake correlates with microvessel density[38] and the proliferative activity,[39] and enables us to differentiate between WHO grade II and WHO grades III/IV gliomas (Fig. 2).[40] By using a threshold of 1.5, [^{11}C]MET-PET permits the differentiation between nontumoral lesions and gliomas with a sensitivity of 79%.[41] However, because of the short half-life of [^{11}C], the use of [^{11}C]MET remains restricted to PET centers with a cyclotron. The nucleoside 3′-deoxy-3′-[^{18}F]fluoro-L-thymidine ([^{18}F]FLT) has recently been investigated as a direct marker for tumor proliferation in vivo.[42] [^{18}F]FLT is carried via specific nucleoside transporters from the blood pool into the brain tissue. Within the cells [^{18}F]FLT reacts as an analogue substrate of thymidine, which is phosphorylated by the thymidine kinase 1 (TK1). TK1 is a cytosolic enzyme that is expressed during the S phase of the cell cycle. TK1 expression is specifically increased in dividing cells and decreased in nondividing cells.[43] Therefore, the assessment of TK1 activity offers a specific target to monitor cell proliferation on the molecular level. Several clinical studies revealed a significant correlation between [^{18}F]FLT uptake and the in vitro proliferation marker K_i-67 in various tumor types.[44–48]

Because of its relatively longer half-life, [^{18}F]FLT enables a detailed kinetic analysis. The use of kinetic modeling enables us to determine the transport rate of [^{18}F]FLT from the blood via the BBB into the tissue (k1) and back into the blood (k2), as well as the phosphorylation rate of [^{18}F]FLT by TK1 (k3) and the dephosphorylation rate of [^{18}F]FLT-monophosphate (k4). In a recent study, we demonstrated that [^{18}F]FLT uptake (1) enables us to differentiate between low-grade and high-grade tumors, and (2) is mainly due to increased transport and to a lower extent to phosphorylation by TK1 in gliomas.[29] Furthermore, the metabolic rate of [^{18}F]FLT as determined by K_i significantly correlates with glioma proliferation as assessed by K_i-67 immunohistochemistry in patients with newly diagnosed high-grade gliomas.[49]

PLANNING OF STEREOTACTIC BIOPSY AND TARGETED APPLICATION OF LOCAL THERAPEUTICS

Noninvasive imaging tools, such as MRI and PET, enable stereotactically guided biopsies to provide histological samples from the most malignant part of the tumor. Stereotactically guided biopsies are highly relevant in the grading of gliomas because of the tumor heterogeneity with different malignant subtypes represented within the same tumor. Since the most malignant part of the tumor mainly drives tumor growth, stereotactic biopsies may provide a more accurate estimation of growth behavior and prognosis. Stereotactic biopsies guided by conventional MRI might miss highly malignant parts of the tumor, since highly proliferating tumor tissue does not necessarily develop contrast enhancement. [^{18}F]FDG PET has been shown to improve the detection of tumor tissue in comparison to anatomical imaging alone.[50] Moreover, as reported recently, [^{11}C]MET is superior to [^{18}F]FDG for guiding stereotactic biopsies because of its high tumor specificity[51] and enables us to detect low proliferating parts of the tumor without contrast enhancement on MRI.[52] Imaging also allows for the local application of targeted therapy approaches, such as radiotherapy, with consequent evaluation of treatment response at follow-up. In a Phase I/II clinical trial, gene therapy vectors have been stereotactically guided and injected into the metabolically active tumor areas by local infusion catheters, enabling us to monitor therapeutic gene expression (Fig. 3).[53]

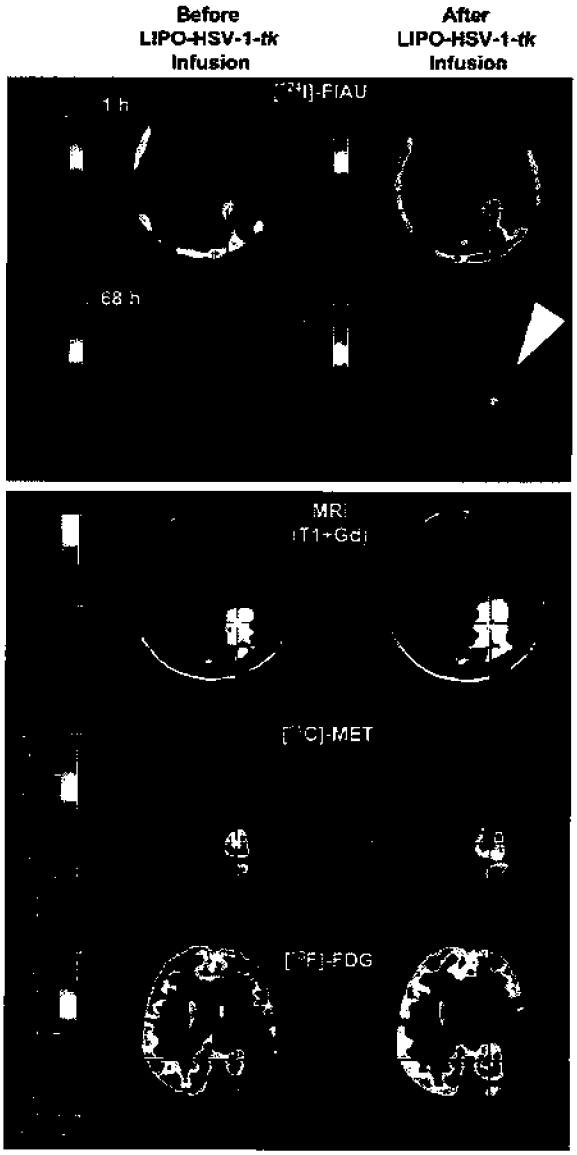

Figure 3 Multimodal imaging for the establishment of imaging-guided experimental treatment strategies. Coregistration of [^{18}F]FIAU-, [^{11}C]MET-, [^{18}F]FDG-PET, and MRI before (left column) and after (right column) targeted application (stereotactic infusion) of a gene therapy vector. The region of specific [^{124}I]-FIAU retention (68 hour) within the tumor after LIPO-HSV-1-*tk* transduction (white arrowhead) resembles the proposed "tissue dose" of vector-mediated gene expression and shows signs of necrosis (cross right column; reduced methionine uptake [MET] and glucose metabolism [FDG]) after ganciclovir treatment. MRI, magnetic resonance imaging. (Reproduced with permission from Jacobs A, Voges J, Reszka R, et al. Positron-emission tomography of vector-mediated gene expression in gene therapy for gliomas. Lancet 2001;358: 727–729.[53])

IMAGING TREATMENT RESPONSE AND DIFFERENTIATION OF RECURRENT TUMOR FROM RADIATION NECROSIS

Monitoring treatment effects is key for the evaluation of new molecular-targeted therapy approaches. Noninvasive imaging allows a rapid assessment of tumor response to potentially guide the best treatment regimen for the individual patient. In particular, promising targeted therapies that affect a specific pathway of tumor growth, such as EGFR inhibitors, require detection of therapeutic response at an early stage of treatment, since only a subpopulation of patients respond to therapy.[54] Thus, one of the major challenges will be the noninvasive differentiation of therapy responders from nonresponders.

Currently, there are limitations in the assessment of therapeutic response in gliomas. Contrast enhancement with MRI reflects highly proliferating tumor tissue. However, contrast enhancement does not allow for the distinction between changes in tumor growth or postsurgical changes. Contrast-enhanced MRI does not enable the interpretation of contrast enhancement 3 days to several weeks after surgery because of operation-induced leakage of the BBB. Moreover, the assessment of changes in tumor size by conventional MRI is usually delayed for months after the start of therapy. Therefore, new imaging protocols have been developed to determine functional characteristics of the tumor.

In an experimental model, early treatment response to BCNU treatment has been assessed by DWI in gliomas.[55] The obtained ADC correlated strongly with survival of the animals and tumor growth delay.[55] In a clinical design, Moffat and associates established a functional diffusion map to provide early prediction of treatment response in patients with brain tumors.[56] Changes in tumor water diffusion were highly predictive of response to therapy 3 weeks after treatment. However, the usefulness of DWI remains limited after dexamethasone treatment, since dexamethasone affects the diffusion with edematous brain[57] and might lead to misleading interpretation of DWI. Furthermore, dynamic contrast-enhanced MRI has been used to monitor antiangiogenic therapies in brain tumors.[58] The vascular endothelial growth factor (VEGF) which is strongly expressed during angiogenesis induces high vascular permeability. Inhibition of VEGF by Avastin treatment—which specifically binds and thereby inhibits VEGF—can be monitored through the kinetic constant K^{trans} obtained by dynamic contrast enhancement in nude rats.[58] New approaches such as volumetric computed tomography allow the detection of tumor vessel with a diameter of 50 μm, enabling the noninvasive evaluation of the angiogenetic environment of tumors.[59] Furthermore, in a clinical MRI study, Batchelor et al observed normalization of tumor vessels in patients with recurrent glioblastoma after VEGF inhibition (AZD2171) by assessing angiogenic characteristics such as vascular permeability (K^{trans}), relative microvessel size, and water diffusion (ADC).[60]

With PET, [^{18}F]FDG has been reported to be not very accurate for the assessment of treatment effects

because of the high cortical background activity.[61,62] In the differentiation between recurrent tumor versus radiation-induced necrosis, [^{18}F]FDG PET revealed a sensitivity of 75% and a specificity of 81%.[63] However, it should be pointed out that [^{18}F]FDG uptake might also be due to migration of macrophages into the tumor, making the interpretation of [^{18}F]FDG uptake difficult for the evaluation of therapy response.[64]

In contrast, [^{11}C]MET-PET shows low background activity in the brain and does not accumulate in macrophages. [^{11}C]MET therefore detects tumor tissue with a high sensitivity (87%) and specificity (89%) by an uptake threshold of 1.3-fold.[37] [^{11}C]MET also enables us to differentiate recurrent tumor from radiation necrosis, while the tracer accumulation is nearly independent from disruption of the BBB or macrophage activity within the necrotic areas.[36] Changes in [^{11}C]MET metabolism assessed with PET indicated a response to temozolomide treatment after three cycles of treatment in gliomas (Fig. 4).[35] However, [^{11}C]MET metabolism

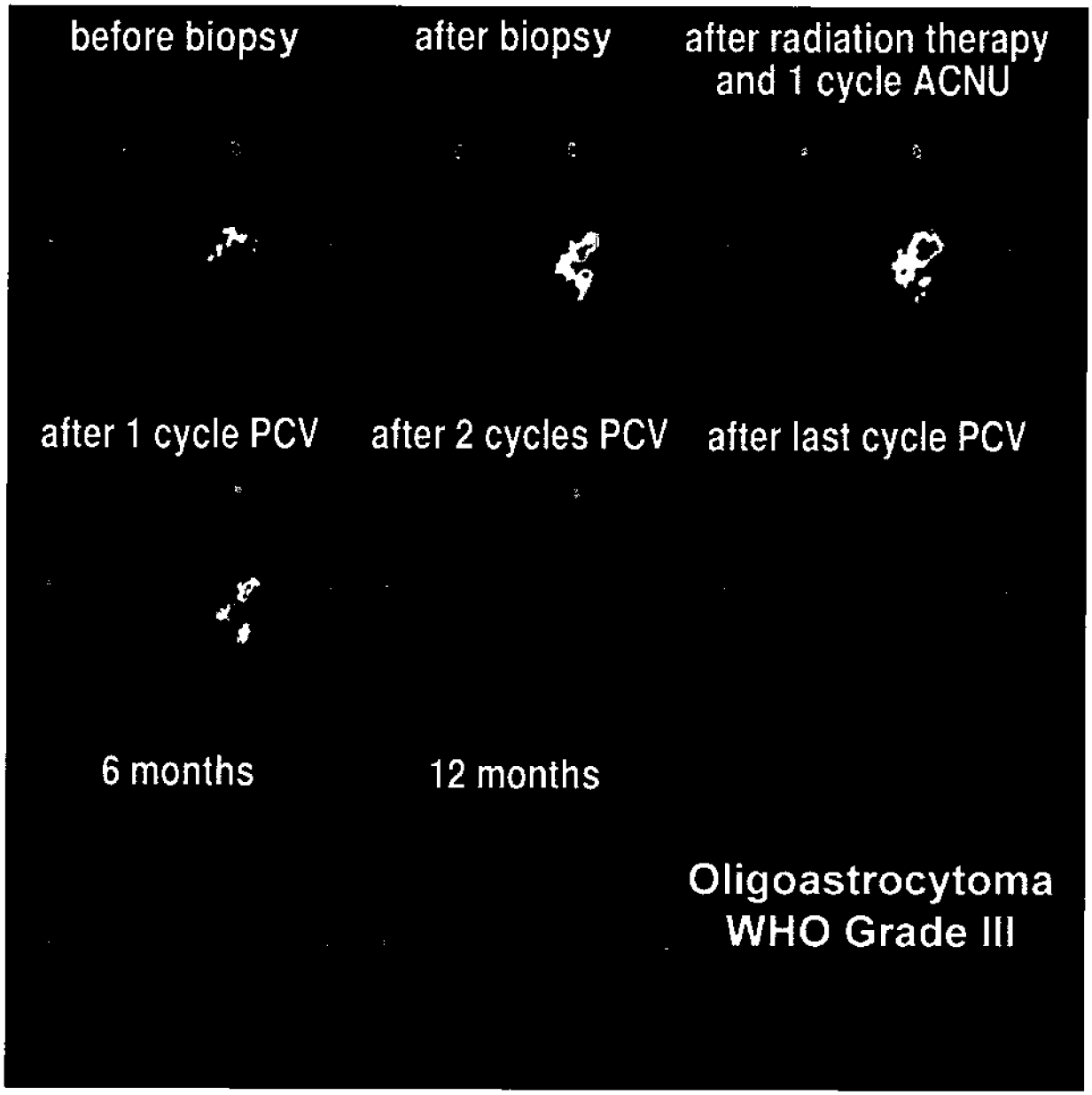

Figure 4 Noninvasive assessment of response to radiotherapy (60 Gy) in combination with ACNU and three cycles of PCV chemotherapy in an oligoastrocytoma, grade III. The [^{11}C]MET-PET image shows high uptake values before and after combined radiotherapy and ACNU treatment. In contrast, [^{11}C]MET uptake significantly decreases after first cycle of PCV treatment and again after the second and the last cycle of PCV treatment. In the follow up investigation after 12 months, the metabolic activity of the glioma remains decreased as assessed by [^{11}C]MET PET. ACNU, nimustin; PCV, procarbazin, CCNU (lomustin), vincristin; PET, positron emission tomography. (Reproduced with permission from Kracht L, Jacobs A, Heiss W. Metabolic Imaging. 2nd ed. Stuttgart: Thieme; 2008:70–78.[75])

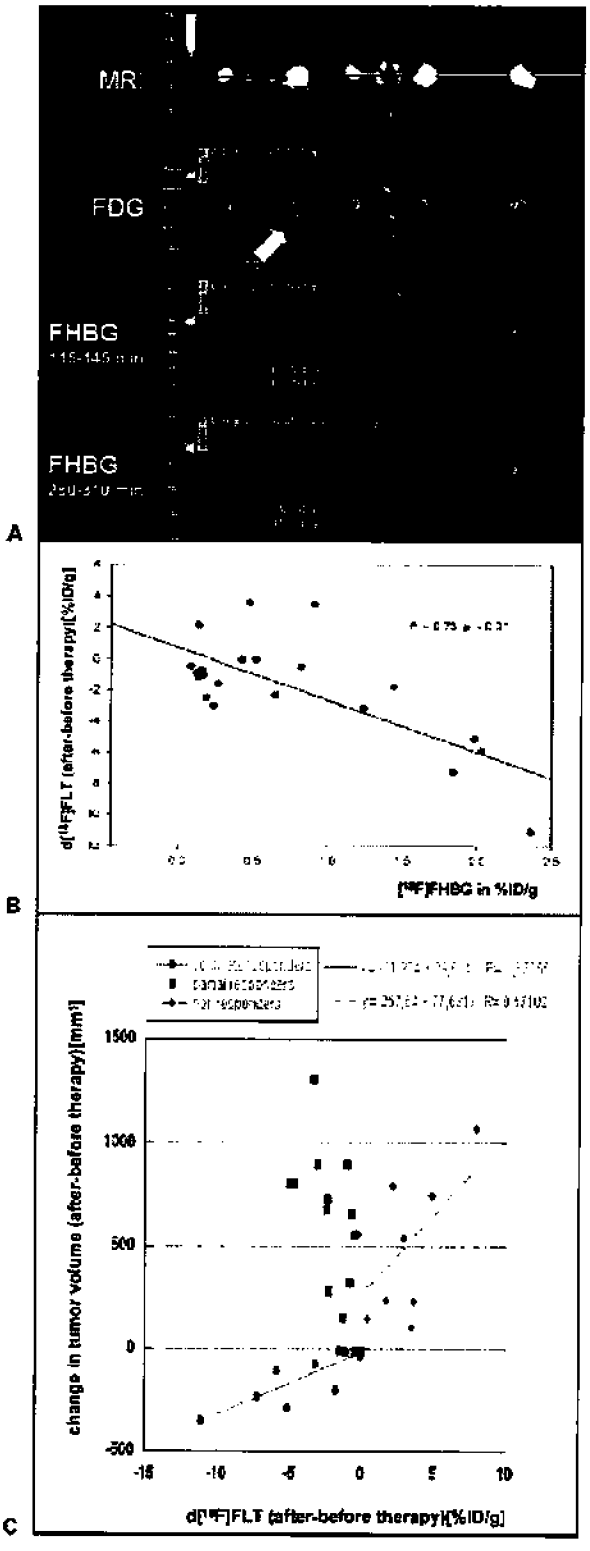

Figure 5 (A) Experimental protocol for identification of viable target tissue and assessment of vector-mediated gene expression in vivo in a mouse model with three subcutaneous gliomas. Row 1: Localization of tumors is displayed by MRI. Row 2: The viable target tissue is displayed by [^{18}F]FDG-PET; note the signs of necrosis in the lateral portion of the left-sided tumor (arrow). Rows 3 and 4: Following vector-application into the medial viable portion of the tumor, the tissue dose of vector-mediated gene expression is quantified by [^{18}F]FHBG-PET. Row 3 shows an image acquired early after tracer injection, which is used for coregistration; row 4 displays a late image with specific tracer accumulation in the tumor that is used for quantification. (B) Response to gene therapy correlates with therapeutic gene expression. The intensity of cdIREStk39 gfp expression, which is equivalent to transduction efficiency and tissue-dose of vector-mediated therapeutic gene expression, is measured by [^{18}F]FHBG-PET (in %ID/g), and the induced therapeutic effect is measured by [^{18}F]FLT-PET ($r = 0.73$, $p < 0.01$). Therapeutic effect ([^{18}F]FLT) was calculated as the difference between [^{18}F]FLT accumulation after and before therapy. (C) Relationship between changes in volumetry and [^{18}F]FLT uptake. Changes in tumor volume and [^{18}F]FLT uptake were plotted for tumors grown in 11 nude mice. There is a strong correlation between volume and change in [^{18}F]FLT uptake ($r = 0.83$) for those tumors responding to therapy (complete responders) and a weaker correlation ($r = 0.57$) for those tumors not responding to therapy (nonresponders). No correlation was found for those tumors where focal alterations of [^{18}F]FLT uptake occurred which did not lead to a reduction in overall tumor volume. MRI, magnetic resonance imaging; PET, positron emission tomography. (Adapted with permission from Jacobs AH, Rueger MA, Winkeler A, et al. Imaging-guided gene therapy of experimental gliomas. Cancer Res 2007;67:1706–1715.[69])

remains a rather indirect marker of proliferation, although correlations with in vitro proliferation have been described recently.[39]

In the field of imaging antiproliferative treatment effects, recent studies demonstrated that changes in [^{18}F]FLT-PET may allow an early assessment of treatment response.[65,66] In recurrent gliomas, changes in [^{18}F]FLT SUV predict overall survival as soon as 1 to 2 weeks after initiation of bevacizmab and irinotecan treatment.[65] However, as mentioned above, [^{18}F]FLT accumulation within the tumor might not only reflect proliferation but also leakage of the BBB. Thus, changes in [^{18}F]FLT uptake have to be considered with caution. Kinetic analysis of tracer distribution within the tissue has to be performed, as it provides more detailed information about the proportion of [^{18}F]FLT uptake that is due to leakage of the BBB and the fraction that is due to phosphorylation of [^{18}F]FLT.[29,49,67,68]

POTENTIAL OF EXPERIMENTAL BRAIN TUMOR IMAGING

Imaging studies in experimental brain tumor models provide: (1) the development of new radiotracers for cellular proliferation and protein synthesis; (2) the evaluation of their ability to detect responses to therapy at an early stage of treatment; (3) strategies for imaging transcriptional regulation and migration of tumor cells;

and (4) a way to monitor the expression of exogenous genes carrying a marker or therapeutic function for the purpose of development of improved gene therapeutic vectors. For imaging-guided vector applications, the biologically active target tissue has to be identified by PET to enable the quantification of the expression of the transduced therapeutic genes in vivo. This should in turn lead to a correlation between transduction efficiency and induced therapeutic effect (Fig. 5).[69,70] Furthermore, labeling agents with tumor-specific antigens such as CD31[71] and the cell adhesion receptor integrin $\alpha(v)\beta(3)$[72,73] provide in vivo characterization of tumor angiogenesis and the noninvasive evaluation of antiangiogenic therapies. Recently, it has been demonstrated that the expression of the cell adhesion receptor integrin $\alpha(v)\beta(3)$ as a marker for angiogenesis can be assessed by MRI and PET.[72,73] This may allow for multimodal imaging of angiogenesis and for the evaluation of antiangiogenic therapy targets in the future.

SUMMARY

Multimodal imaging strategies provide a better understanding of the pathophysiology and molecular alterations of brain tumors. In the clinical arena, molecular imaging techniques have been established to (1) detect brain tumor with a high sensitivity and specificity, (2) evaluate the grade of malignancy, and (3) assess therapy response, even on a molecular targeted level. Highly promising imaging techniques that specifically assess molecular cancer characteristics, such as angiogenesis or deregulation of the cell cycle, remain to be validated in a clinical setting. This might enable us to monitor therapy strategies that address specific molecular targets. Finally, noninvasive imaging after therapy will improve drug development and facilitate the early assessment of treatment effects in the future.

ACKNOWLEDGMENTS

This work is supported in part by the Ministerium für Schule, Wissenschaft und Forschung NRW (MSWF 516–40000299), the Center for Molecular Medicine Cologne (CMMC-TV46), the Max-Planck Society, Germany, 6th FW EU grant EMIL (LSHC-CT-2004–503569) EC-FP6-Project DiMI: LSHB-CT-2005–512146, and EC-FP6-Clinigene: LSBH-CT-06–018933.

REFERENCES

1. Louis DN, Ohgaki H, Wiestler OD, et al. The 2007 WHO classification of tumours of the central nervous system. Acta Neuropathol 2007;114:97–109
2. Watanabe K, Sato K, Biernat W, et al. Incidence and timing of p53 mutations during astrocytoma progression in patients with multiple biopsies. Clin Cancer Res 1997;3:523–530
3. Bogler O, Huang HJ, Kleihues P, Cavenee WK. The p53 gene and its role in human brain tumors. Glia 1995;15:308–327
4. Watanabe T, Katayama Y, Yoshino A, Komine C, Yokoyama T. Deregulation of the TP53/p14ARF tumor suppressor pathway in low-grade diffuse astrocytomas and its influence on clinical course. Clin Cancer Res 2003;9:4884–4890
5. Momand J, Zambetti GP, Olson DC, George D, Levine AJ. The mdm-2 oncogene product forms a complex with the p53 protein and inhibits p53-mediated transactivation. Cell 1992;69:1237–1245
6. Kamijo T, Weber JD, Zambetti G, Zindy F, Roussel MF, Sherr CJ. Functional and physical interactions of the ARF tumor suppressor with p53 and Mdm2. Proc Natl Acad Sci U S A 1998;95:8292–8297
7. Ohgaki H, Dessen P, Jourde B, et al. Genetic pathways to glioblastoma: a population-based study. Cancer Res 2004;64:6892–6899
8. Cairncross JG, Ueki K, Zlatescu MC, et al. Specific genetic predictors of chemotherapeutic response and survival in patients with anaplastic oligodendrogliomas. J Natl Cancer Inst 1998;90:1473–1479
9. Mellinghoff IK, Wang MY, Vivanco I, et al. Molecular determinants of the response of glioblastomas to EGFR kinase inhibitors. N Engl J Med 2005;353:2012–2024
10. Scott JN, Brasher PM, Sevick RJ, Rewcastle NB, Forsyth PA. How often are nonenhancing supratentorial gliomas malignant? A population study. Neurology 2002;59:947–949
11. Sugahara T, Korogi Y, Kochi M, et al. Usefulness of diffusion-weighted MRI with echo-planar technique in the evaluation of cellularity in gliomas. J Magn Reson Imaging 1999;9:53–60
12. Pauleit D, Langen KJ, Floeth F, et al. Can the apparent diffusion coefficient be used as a noninvasive parameter to distinguish tumor tissue from peritumoral tissue in cerebral gliomas? J Magn Reson Imaging 2004;20:758–764
13. Sugahara T, Korogi Y, Kochi M, et al. Correlation of MR imaging-determined cerebral blood volume maps with histologic and angiographic determination of vascularity of gliomas. AJR Am J Roentgenol 1998;171:1479–1486
14. Aronen HJ, Gazit IE, Louis DN, et al. Cerebral blood volume maps of gliomas: comparison with tumor grade and histologic findings. Radiology 1994;191:41–51
15. Maia AC Jr, Malheiros SM, da Rocha AJ, et al. MR cerebral blood volume maps correlated with vascular endothelial growth factor expression and tumor grade in nonenhancing gliomas. AJNR Am J Neuroradiol 2005;26:777–783
16. Hakyemez B, Erdogan C, Bolca N, et al. Evaluation of different cerebral mass lesions by perfusion-weighted MR imaging. J Magn Reson Imaging 2006;24:817–824
17. Roberts HC, Roberts TP, Brasch RC, Dillon WP. Quantitative measurement of microvascular permeability in human brain tumors achieved using dynamic contrast-enhanced MR imaging: correlation with histologic grade. AJNR Am J Neuroradiol 2000;21:891–899
18. Law M, Yang S, Babb JS, et al. Comparison of cerebral blood volume and vascular permeability from dynamic susceptibility contrast-enhanced perfusion MR imaging with glioma grade. AJNR Am J Neuroradiol 2004;25:746–755

19. Law M, Yang S, Wang H, et al. Glioma grading: sensitivity, specificity, and predictive values of perfusion MR imaging and proton MR spectroscopic imaging compared with conventional MR imaging. AJNR Am J Neuroradiol 2003; 24:1989–1998
20. Moller-Hartmann W, Herminghaus S, Krings T, et al. Clinical application of proton magnetic resonance spectroscopy in the diagnosis of intracranial mass lesions. Neuroradiology 2002;44:371–381
21. Ishimaru H, Morikawa M, Iwanaga S, et al. Differentiation between high-grade glioma and metastatic brain tumor using single-voxel proton MR spectroscopy. Eur Radiol 2001;11: 1784–1791
22. Oshiro S, Tsugu H, Komatsu F, et al. Quantitative assessment of gliomas by proton magnetic resonance spectroscopy. Anticancer Res 2007;27:3757–3763
23. Zhao S, Kuge Y, Mochizuki T, et al. Biologic correlates of intratumoral heterogeneity in 18F-FDG distribution with regional expression of glucose transporters and hexokinase-II in experimental tumor. J Nucl Med 2005;46:675–682
24. Bos R, van Der Hoeven JJ, van Der Wall E, et al. Biologic correlates of (18)fluorodeoxyglucose uptake in human breast cancer measured by positron emission tomography. J Clin Oncol 2002;20:379–387
25. Herholz K, Pietrzyk U, Voges J, et al. Correlation of glucose consumption and tumor cell density in astrocytomas. A stereotactic PET study. J Neurosurg 1993;79:853–858
26. Herholz K, Heindel W, Luyten PR, et al. In vivo imaging of glucose consumption and lactate concentration in human gliomas. Ann Neurol 1992;31:319–327
27. Di Chiro G, DeLaPaz RL, Brooks RA, et al. Glucose utilization of cerebral gliomas measured by [18F] fluorodeoxyglucose and positron emission tomography. Neurology 1982;32:1323–1329
28. Alavi JB, Alavi A, Chawluk J, et al. Positron emission tomography in patients with glioma. A predictor of prognosis. Cancer 1988;62:1074–1078
29. Jacobs AH, Thomas A, Kracht LW, et al. 18F-fluoro-L-thymidine and 11C-methylmethionine as markers of increased transport and proliferation in brain tumors. J Nucl Med 2005;46:1948–1958
30. Jager PL, Vaalburg W, Pruim J, et al. Radiolabelled amino acids: basic aspects and clinical applications in oncology. J Nucl Med 2001;42:432–445
31. Pauleit D, Floeth F, Tellmann L, et al. Comparison of O-(2–18F-fluoroethyl)-L-tyrosine PET and 3–123I-iodo-alpha-methyl-L-tyrosine SPECT in brain tumors. J Nucl Med 2004;45:374–381
32. Miyagawa T, Oku T, Uehara H, et al. "Facilitated" amino acid transport is upregulated in brain tumors. J Cereb Blood Flow Metab 1998;18:500–509
33. Bergstrom M, Lundqvist H, Ericson K, et al. Comparison of the accumulation kinetics of L-(methyl-11C)-methionine and D-(methyl-11C)-methionine in brain tumors studied with positron emission tomography. Acta Radiol 1987;28: 225–229
34. Van Laere K, Ceyssens S, Van Calenbergh F, et al. Direct comparison of 18F-FDG and 11C-methionine PET in suspected recurrence of glioma: sensitivity, inter-observer variability and prognostic value. Eur J Nucl Med Mol Imaging 2005;32:39–51
35. Galldiks N, Kracht LW, Burghaus L, et al. Use of 11C-methionine PET to monitor the effects of temozolomide chemotherapy in malignant gliomas. Eur J Nucl Med Mol Imaging 2006;33:516–524
36. Thiel A, Pietrzyk U, Sturm V, et al. Enhanced accuracy in differential diagnosis of radiation necrosis by positron emission tomography–magnetic resonance imaging coregistration: technical case report. Neurosurgery 2000;46: 232–234
37. Kracht LW, Miletic H, Busch S, et al. Delineation of brain tumor extent with [11C]L-methionine positron emission tomography: local comparison with stereotactic histopathology. Clin Cancer Res 2004;10:7163–7170
38. Kracht LW, Friese M, Herholz K, et al. Methyl-[11C]- l-methionine uptake as measured by positron emission tomography correlates to microvessel density in patients with glioma. Eur J Nucl Med Mol Imaging 2003;30:868–873
39. Sato N, Suzuki M, Kuwata N, et al. Evaluation of the malignancy of glioma using 11C-methionine positron emission tomography and proliferating cell nuclear antigen staining. Neurosurg Rev 1999;22:210–214
40. Sasaki M, Kuwabara Y, Yoshida T, et al. A comparative study of thallium-201 SPECT, carbon-11 methionine PET and fluorine-18 fluorodeoxyglucose PET for the differentiation of astrocytic tumours. Eur J Nucl Med 1998;25: 1261–1269
41. Herholz K, Holzer T, Bauer B, et al. 11C-methionine PET for differential diagnosis of low-grade gliomas. Neurology 1998;50:1316–1322
42. Shields AF, Grierson JR, Dohmen BM, et al. Imaging proliferation in vivo with [F-18]FLT and positron emission tomography. Nat Med 1998;4:1334–1336
43. Sherley JL, Kelly TJ. Regulation of human thymidine kinase during the cell cycle. J Biol Chem 1988;263:8350–8358
44. Vesselle H, Grierson J, Muzi M, et al. In vivo validation of 3'deoxy-3'-[(18)F]fluorothymidine ([(18)F]FLT) as a proliferation imaging tracer in humans: correlation of [(18)F]FLT uptake by positron emission tomography with Ki-67 immunohistochemistry and flow cytometry in human lung tumors. Clin Cancer Res 2002;8:3315–3323
45. Wells P, Gunn RN, Alison M, et al. Assessment of proliferation in vivo using 2-[(11)C]thymidine positron emission tomography in advanced intra-abdominal malignancies. Cancer Res 2002;62:5698–5702
46. Buck AK, Bommer M, Stilgenbauer S, et al. Molecular imaging of proliferation in malignant lymphoma. Cancer Res 2006;66:11055–11061
47. Buck AK, Schirrmeister H, Hetzel M, et al. 3-deoxy-3-[(18)F]fluorothymidine-positron emission tomography for noninvasive assessment of proliferation in pulmonary nodules. Cancer Res 2002;62:3331–3334
48. Wagner M, Seitz U, Buck A, et al. 3'-[18F]fluoro-3'-deoxythymidine ([18F]-FLT) as positron emission tomography tracer for imaging proliferation in a murine B-Cell lymphoma model and in the human disease. Cancer Res 2003; 63:2681–2687
49. Ullrich R, Backes H, Li HF, et al. Glioma proliferation as assessed by FLT-PET in patients with newly diagnosed high grade glioma. Clin Cancer Res 2008;14:2049–2055
50. Levivier M, Goldman S, Pirotte B, et al. Diagnostic yield of stereotactic brain biopsy guided by positron emission tomography with [18F]fluorodeoxyglucose. J Neurosurg 1995;82: 445–452
51. Pirotte B, Goldman S, Massager N, et al. Combined use of 18F-fluorodeoxyglucose and 11C-methionine in 45 positron

emission tomography-guided stereotactic brain biopsies. J Neurosurg 2004;101:476–483
52. Gumprecht H, Grosu AL, Souvatsoglou M, et al. 11C-Methionine positron emission tomography for preoperative evaluation of suggestive low-grade gliomas. Zentralbl Neurochir 2007;68:19–23
53. Jacobs A, Voges J, Reszka R, et al. Positron-emission tomography of vector-mediated gene expression in gene therapy for gliomas. Lancet 2001;358:727–729
54. Sequist LV, Bell DW, Lynch TJ, Haber DA. Molecular predictors of response to epidermal growth factor receptor antagonists in non–small-cell lung cancer. J Clin Oncol 2007; 25:587–595
55. Lee KC, Hall DE, Hoff BA, et al. Dynamic imaging of emerging resistance during cancer therapy. Cancer Res 2006;66:4687–4692
56. Moffat BA, Chenevert TL, Lawrence TS, et al. Functional diffusion map: a noninvasive MRI biomarker for early stratification of clinical brain tumor response. Proc Natl Acad Sci U S A 2005;102:5524–5529
57. Sinha S, Bastin ME, Wardlaw JM, Armitage PA, Whittle IR. Effects of dexamethasone on peritumoural oedematous brain: a DT-MRI study. J Neurol Neurosurg Psychiatry 2004;75:1632–1635
58. Gossmann A, Helbich TH, Kuriyama N, et al. Dynamic contrast-enhanced magnetic resonance imaging as a surrogate marker of tumor response to anti-angiogenic therapy in a xenograft model of glioblastoma multiforme. J Magn Reson Imaging 2002;15:233–240
59. Kiessling F, Greschus S, Lichy MP, et al. Volumetric computed tomography (VCT): a new technology for non-invasive, high-resolution monitoring of tumor angiogenesis. Nat Med 2004;10:1133–1138
60. Batchelor TT, Sorensen AG, di Tomaso E, et al. AZD2171, a pan-VEGF receptor tyrosine kinase inhibitor, normalizes tumor vasculature and alleviates edema in glioblastoma patients. Cancer Cell 2007;11:83–95
61. Kim EE, Chung SK, Haynie TP, et al. Differentiation of residual or recurrent tumors from post-treatment changes with F-18 FDG PET. Radiographics 1992;12:269–279
62. Wurker M, Herholz K, Voges J, et al. Glucose consumption and methionine uptake in low-grade gliomas after iodine-125 brachytherapy. Eur J Nucl Med 1996;23:583–586
63. Chao ST, Suh JH, Raja S, Lee SY, Barnett G. The sensitivity and specificity of FDG PET in distinguishing recurrent brain tumor from radionecrosis in patients treated with stereotactic radiosurgery. Int J Cancer 2001;96:191–197
64. Reinhardt MJ, Kubota K, Yamada S, Iwata R, Yaegashi H. Assessment of cancer recurrence in residual tumors after fractionated radiotherapy: a comparison of fluorodeoxyglucose, L-methionine and thymidine. J Nucl Med 1997;38: 280–287
65. Chen W, Delaloye S, Silverman DH, et al. Predicting treatment response of malignant gliomas to bevacizumab and irinotecan by imaging proliferation with [18F] fluorothymidine positron emission tomography: a pilot study. J Clin Oncol 2007;25:4714–4721
66. Herrmann K, Wieder HA, Buck AK, et al. Early response assessment using 3′-deoxy-3′-[18F]fluorothymidine-positron emission tomography in high-grade non-Hodgkin's lymphoma. Clin Cancer Res 2007;13:3552–3558
67. Muzi M, Spence AM, O'Sullivan F, et al. Kinetic analysis of 3′-deoxy-3′-18F-fluorothymidine in patients with gliomas. J Nucl Med 2006;47:1612–1621
68. Schiepers C, Chen W, Dahlbom M, et al. 18F-fluorothymidine kinetics of malignant brain tumors. Eur J Nucl Med Mol Imaging 2007;34:1003–1011
69. Jacobs AH, Rueger MA, Winkeler A, et al. Imaging-guided gene therapy of experimental gliomas. Cancer Res 2007;67: 1706–1715
70. Winkeler A, Sena-Esteves M, Paulis LE, et al. Switching on the lights for gene therapy. PLoS ONE 2007;2:e528
71. McAteer MA, Sibson NR, von Zur Muhlen C, et al. In vivo magnetic resonance imaging of acute brain inflammation using microparticles of iron oxide. Nat Med 2007;13:1253–1258
72. Mulder WJ, van der Schaft DW, Hautvast PA, et al. Early in vivo assessment of angiostatic therapy efficacy by molecular MRI. FASEB J 2007;21:378–383
73. Beer AJ, Lorenzen S, Metz S, et al. Comparison of integrin alphaVbeta3 expression and glucose metabolism in primary and metastatic lesions in cancer patients: a PET study using 18F-galacto-RGD and 18F-FDG. J Nucl Med 2008; 49:22–29
74. Jacobs A. PET in Gliomas. Stuttgart: Thieme; 2003:72–76
75. Kracht L, Jacobs A, Heiss W. Metabolic Imaging. 2nd ed. Stuttgart: Thieme; 2008:70–78